

A theoretical approach towards digital twins

**A balance between an empirical and a
fundamental model for distribution
transformers**

by

M. van Dijk

to obtain the degree of Master of Science
at the Delft University of Technology,
to be defended publicly on Wednesday 16 February 2022 at 10:00.

Student number: 4584252
Project duration: 1 April 2021 – 19 January 2022
Thesis committee: Dr. D. J. P. Lahaye, TU Delft, supervisor
Dr. J. D. Schuddebeurs, Stedin, supervisor
Dr. ir. M. B. Van Gijzen, TU Delft

An electronic version of this thesis is available at <http://repository.tudelft.nl/>.



Abstract

The energy transition will significantly impact distribution transformers as they will have to deal with more load on them, which is also more variable due to renewable energy sources. However, currently, these transformers are often not monitored with sensors. Therefore, the Dutch network operator Stedin asked to investigate the possibilities of a digital twin for distribution transformers without many sensors. This thesis presents two ways to do so: the currently most used but more empirical loading guide and a more analytical method where we solve Maxwell's equations using the finite element method (FEM). Furthermore, the transition to more renewable energy sources and sources that draw instant power from the grid causes the current to get distorted. This distortion can be mathematically analyzed using harmonic functions, and we will consider the impact of these harmonics in both the loading guide and the FEM model.

The loading guide is a method written in slightly different ways in the IEEE and IEC standards that takes the load on a transformer and the ambient temperature around the transformer to determine the hot spot temperature inside the transformer. By saying that the hot spot temperature is the warmest point inside the transformer, we can determine the percentage of loss of life of a transformer for a particular loading pattern. However, the loading guide only considers one set of parameter values for distribution transformers, which can vary widely in rating, location and ventilation household, leading to an over-or underestimation of the temperature, which in both cases can lead to extra costs. Additionally, the impact of harmonics is an empirical addition to the loading guide and only considers the effect on temperature rise and not the losses.

Therefore, we consider the transformer in a finite element approach. We solve Maxwell's equation on a transformer cross-section with the FEM, resulting in a 2D model that can calculate the losses for a particular geometry. This model is made using COMSOL Multiphysics®. Furthermore, we calculate the core and winding losses under a harmonic load, resulting in considerably higher losses than without harmonics.

As the FEM model is quick and straightforward to run, it can serve as a first step towards developing a digital twin of distribution transformer, giving a way to determine the losses analytically. With future development, the model can provide better insight into the temperature distribution in the transformer.

Preface

Before you lies my master thesis, “A theoretical approach towards digital twins: A balance between an empirical and a fundamental model for distribution transformers”, marking the end of my 5.5 year period at the TU Delft. For this project, I looked at two methods to determine the condition of distribution transformers: the loading guide and an analytical model which solves Maxwell’s equations using the finite element method (FEM). The approach of using a FEM for transformer monitoring is new, and therefore it will be presented at the 2022 SCEE conference, for which the reader can find the submitted 1-page abstract in Appendix C.

This research started with a question from and was performed in collaboration with Stedin, and I would therefore want to thank them for their support and expertise. First, I would like to thank Jan Stedehouder for coming up with this assignment and supervising me throughout. Second, I would like to thank Jeroen Schuddebeurs for guiding me and emphasizing the potential of this project within Stedin.

From the TU Delft, I would like to thank Domenico Lahaye for his guidance and our sometimes hour-long meetings where we discussed the model to see how we could improve it. Additionally, I would like to thank Martin van Gijzen for being part of the thesis committee.

Lastly, I want to thank my friends and family for their continued support.

*M. van Dijk
Delft, January 2022*

Contents

1	Introduction	1
1.1	Research theme	1
1.2	Digital twins.	1
1.3	Research goals	3
1.4	Outline.	4
2	Introduction to distribution transformers	5
2.1	Basics electricity network.	5
2.2	Components in a distribution network	8
2.3	Types of transformers	9
2.4	Workings	9
2.5	Components	10
2.6	Harmonics	15
2.7	Current asset management	17
3	The behaviour of a transformer	18
3.1	Losses.	18
3.2	Physics inside a transformer	20
3.2.1	Heat.	21
3.2.2	Solid mechanics.	21
4	The loading guide	22
4.1	Transformer life loss calculation.	23
4.2	IEEE loading guide	24
4.3	IEC loading guide	25
4.4	Example loading guides	27
4.5	Including harmonics	29
4.6	Conclusion loading guide.	33
5	Theoretical background first principles model	34
5.1	Study types	35
5.2	Coil excitation	38
5.3	Constitutive parameters	39
5.3.1	B-H relation	40
5.3.2	Conductivity	41
5.4	Losses.	42
5.5	Heating	44
6	Model runs	45
6.1	Geometry	45
6.2	Mesh.	46
6.3	Coil excitation and material coefficients	46
6.4	Core loss	50
6.5	Winding loss	51
6.6	Harmonics	53

7 Discussion & recommendations	58
7.1 Discussion	58
7.2 Recommendations	58
7.2.1 Future research	58
7.2.2 For Stedin	60
8 Conclusion	62
Bibliography	64
A Dataset example Loading Guide	69
B Complex losses	71
C Abstract presented at SCEE conference	72

1

Introduction

1.1. Research theme

Our energy supply is changing from burning fossil fuels in coal power plants and gasoline cars to generating energy with solar panels, heat pumps, and electric vehicles [1]. For the companies that manage the electricity distribution, like Stedin, this shift comes with enormous challenges: more wind turbines and solar panels cause more variable loads, while more heat pumps, induction plates, and electric cars cause a massive increase in the load that travels through the grid. The problem is that the infrastructural investments to deal with these issues can not keep up with the pace of the energy transition [2]. This means that the assets currently in the grid will be prone to more loads, which are harder to predict, as they can also become more variable.

For this research, conducted in collaboration with Stedin, we will look at the effect the energy transition has on the condition and lifetime of distribution transformers. Distribution transformers are located in every neighbourhood, playing a vital role in the energy transition. For example, more solar panels on roofs make the load more variable, and more electric cars and heat pumps increase the load on the transformers [3]. Previously, when companies like Stedin placed distribution transformers, they were only checked minimally by them. It was assumed that little to no maintenance needed to be done on them, as there are no moving parts inside these transformers.

However, these transformers are more likely to be put under higher loads than they were rated for because of the energy transition. Furthermore, they have to deal with new phenomena such as harmonics. We will explain this term in Section 2.6, with both aspects reducing their remaining life faster than what transformer manufacturer designed them for. The life span is highly influenced by the temperature inside it, as with higher temperatures, the insulation material breaks down, increasing the chances of a short circuit [4]. This asset life cycle has been studied quite thoroughly for the high voltage transformers, which are more capital intensive. The research on low distribution transformers still leaves a lot to be desired.

1.2. Digital twins

For this research, we will look at the lifetime evolution of distribution transformers in the context of digital twins [5]. Modelling the asset life cycle and behaviour of distribution transformers under the changing patterns of energy use and distribution is one area where a digital twin can be helpful.

A digital twin is a digital representation of the physical world, which is fed with (near) real-time data to evaluate the object's current state and to make predictions about what will happen to the object in the future [6]. One of the advantages of digital twins is that one can test a proposed change beforehand and see the results. Making a change in a digital copy is more efficient than making that change in the real world first and later seeing that the result is unsatisfactory. For example, a digital twin of the electricity grid might look as follows: say the government has plans for a new neighbourhood, with all houses having solar panels and electric cars. Then, their plans can be put into a digital twin, showing the effects of their plans on the current electricity grid and what the impact will be if we make specific improvements to the grid. The TU Delft has recently developed this sort of digital twin [7].

Stedin is still looking at what kind of digital twins they want to incorporate in their operation and in what areas they already have a basis for a digital twin. Therefore, this research will cover an area where Stedin does not have a digital twin, namely, an asset-based digital twin. As mentioned before, for a digital twin, real-time object data is needed. The problem is: Stedin does not have this data for a lot of their assets, and this is also where their original research question came from:

How can we model assets of our electricity grid in a digital twin for which we do not know their exact condition and behaviour?

For this research, we narrowed the question down to consider the behaviour of distribution transformers. Distribution transformers are an interesting asset to study because newly developed electronics such as LED lights and solar panels generate harmonics that impact a distribution transformer's workings and remaining life. However, it is unclear what effect these electronics precisely have. Also, Stedin has more than 25.000 distribution transformers, all from different manufacturers and build years, leading to slightly different lifetimes, as illustrated in Figure 1.1.

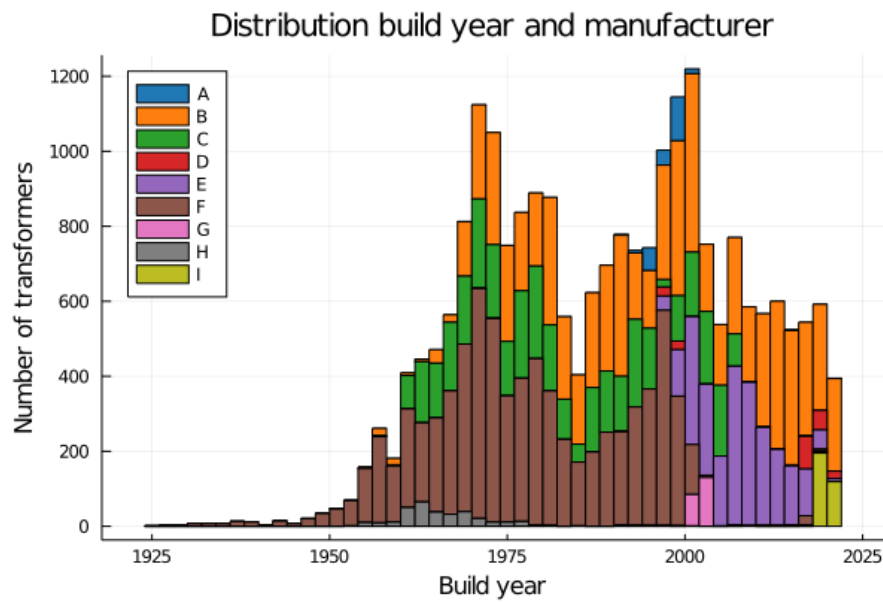


Figure 1.1: Distribution of build year and manufacturer of Stedin's distribution transformers (anonymized for protection of intellectual property)

Currently, Stedin is working on implementing sensors in the stations where they placed their distribution transformers, but this will take another ten years to be fully operational. Recently, the idea of a digital twin for transformers has come up at other research institutes such as MIT Portugal, where they are creating a digital twin of a power transformer [8]. However, they base this digital twin on newly developed transformers, whereas Stedin would like to say something about transformers currently in operation.

There are different ways of constructing a digital twin [9]. One such approach is an entirely data-driven approach where the data from sensors is the input for machine learning models. With these models, we can estimate the current state of the transformer and predict what will happen to that object in the future. On the other hand, there is a physics-driven approach. In this case, we can determine the object's state by the physical equations describing the object's behaviour, and by using, for example, a finite element method (FEM), we can numerically analyze these equations to determine the condition of the object under certain circumstances [10]. A combination of a data-driven and physics-based digital twin is also possible with the help of a Kalman Filter. A Kalman Filter uses a physical model, update this model with real-time data, and predict what will happen in the future with the basis of the physical model [11].

Without a lot of real-time data, we can only develop an asset-based digital twin to predict the remaining life in one way: a physics-based digital twin, where the twin is a physical model. We will look at two approaches for this physical model: the loading guide, which was developed for power transformers, and a more fundamental model based on Maxwell's equations and the finite element method.

To materialize both these models, we will work with a specific case of a distribution transformer for which Stedin already has some real-time data, namely a pair of transformers in The Hague. Besides other variables, Stedin measures the load on each transformer, which we can use as input for the loading guide. For the more fundamental approach, we will need more detailed knowledge about the parts of the transformer we are studying and its dimensions. Transformer manufacturer IEO supplied these two components. They also provided schematic drawings of the inside of their transformer and more detailed measurements about the losses and temperature rise of the transformer.

1.3. Research goals

The loading guide is the current go-to method to determine the remaining life of a transformer. It relies on the fact that a higher temperature causes the paper insulation in a transformer to deteriorate, meaning that a higher temperature shortens the lifetime. The loading guide contains three differential equations that use the load on the transformer and ambient temperature around the transformer as input to determine the hot spot temperature. Then with this hot spot temperature, the loss of life is determined.

For the finite element method, we take one step back and ask ourselves: where is the heat in a transformer coming from? The heat is coming from losses occurring in the electromagnetic process in a transformer. When harmonic currents are present, the losses will increase, causing the temperature to rise.

With both these models at hand, we can formulate multiple research questions:

- As the loading guide was developed for power transformers, what does it say about distribution transformers?
- How can we use a more analytical approach, such as Maxwell's equations, to determine the remaining life of distribution transformers?

- How do the loading guide and the finite element-based method compare to one another in determining the remaining life of a distribution transformer?
- How do the loading guide and the first principles model fit into the area of digital twins?

1.4. Outline

The next chapter introduces the electricity grid, for which we introduce useful mathematical concepts. Additionally, the components in the electricity grid are discussed, with a more detailed look at transformers. Then, in Chapter 3, we dive deeper into the behaviour of the transformer and describe what physics takes place in a transformer. In Chapter 4, we describe and discuss the loading guide and give an example of its potential use. Next, in Chapter 5, we provide the theoretical background for the developed model in Chapter 6. Then, in Chapter 7, we discuss the findings and give recommendations to further develop the model and provide recommendations for Stedin to monitor their transformers. Lastly, Chapter 8 shortly summarizes the results and discussion.

As a last remark, we will present this research at the SCEE 2022 conference, and the reader can find the submitted abstract in Appendix C.

2

Introduction to distribution transformers

Transformers are one of the most vital components in electricity networks. They allow us to transport electricity, generated in a power plant far away, to our houses, without losing much of the generated power. The idea behind transformers is the following: say a power plant generates 100kW of power at $220V$, giving a current of $50.000/220 = 227.27A$. Losses occur when this power is transported through a line, given by $P_{loss} = I^2R$, where R is the resistance of the wire. By taking the resistance of an overhead power line, $R = 0.03$, the losses would be equal to $P_{loss} = 1549.58W$, so around 3% of the generated power is lost in transmission. Transformers enable us to increase the voltage at the power plant and decrease it again when it enters the neighbourhood. Thus, if we transform the power to have $10kV$ instead of $220V$, the losses will be equal to $0.75W$, or only 0.0015% of the generated power.

To further explain why transformers are so essential to our electricity grid, we first need to get a basic idea of how our electricity grid works. We will explain this in the next section. After that, we give the different types of transformers an overview of their components and their basic workings. Lastly, we describe the current state of asset management for these transformers.

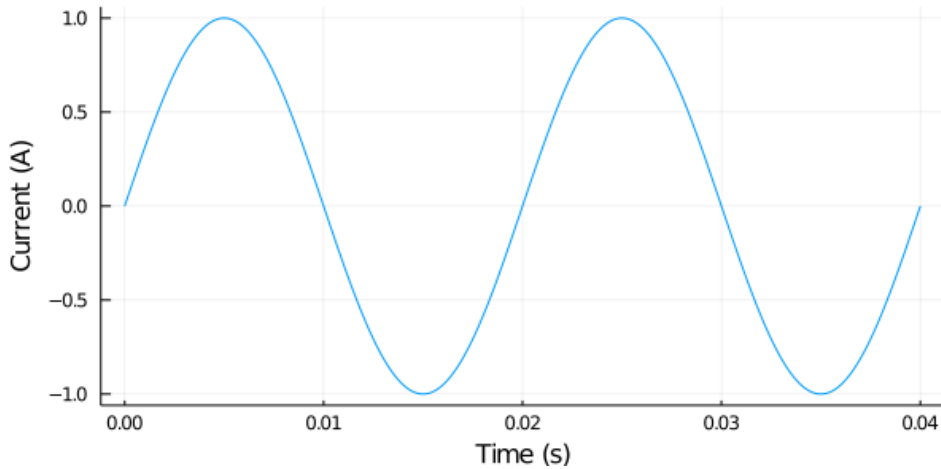
2.1. Basics electricity network

Before we explain the workings and components of a transformer, we will list some definitions for the core components of the electricity grid. First of all, a current in a wire is the amount of charge per unit time passing a given point, given in ampere (A) [12]. The electricity grid is designed so that the current travelling through the electricity cables alternates [13]. This alternating current (AC) is an electric charge that moves back and forth between two points. The idea behind AC is that less of the generated electricity is lost during transmission since we can transform it to higher and lower voltages with transformers. Voltage is the force needed to move the electric charge from one point to another, given in volts (V).

Mathematically an alternating current can be described by a sinusoidal function, which has a frequency, amplitude and phase, as visualized in Figure 2.1 and which can be mathematically described by:

$$i(t) = \hat{i} \sin(\omega t + \psi_I) \quad (2.1)$$

Where \hat{i} is the amplitude of the current, $\omega = 2\pi f$ is the angular frequency, f is the frequency (in Hz), and ψ_I is the phase shift (in radians). For example, in Europe, the electricity grid operates with a current frequency of 50Hz.

Figure 2.1: Sinusoidal current at 50Hz with $\hat{i} = 1A$

Besides the current, we also have an alternating voltage. A sinusoidal function also describes the voltage, but this time with a different phase shift and amplitude:

$$u(t) = \hat{u} \sin(\omega t + \psi_U) \quad (2.2)$$

where \hat{u} is the amplitude of the voltage, and ψ_U is the phase angle (in radians). ¹

As shown above, both the current and voltage vary between positive and negative values. However, for we just want one value to indicate how much current and voltage our appliances use. This is given by the root mean square (RMS) of the current (and voltage). The RMS current is the time average of the current and is mathematically given by:

$$I_{rms} = \sqrt{\frac{1}{T} \int_0^T [\hat{i} \sin(\omega t + \psi_I)]^2 dt} \quad (2.3)$$

$$= \hat{i} \sqrt{\frac{1}{2T} \int_0^T [1 - \cos(2\omega t + 2\psi_I)] dt} \quad (2.4)$$

$$= \hat{i} \sqrt{\frac{1}{2T} \int_0^T dt} \quad (2.5)$$

$$= \frac{\hat{i}}{\sqrt{2}} \quad (2.6)$$

And similarly for the voltage: $U_{rms} = \frac{\hat{u}}{\sqrt{2}}$

We can multiply the equations for the current and voltage, giving the power generated by the current and voltage:

$$p(t) = i(t)u(t) = \hat{i}\hat{u} \sin(\omega t + \psi_I) \sin(\omega t + \psi_U) \quad (2.7)$$

$$= \frac{1}{2} \hat{i}\hat{u} (\cos(\psi_I - \psi_U) - \cos(\psi_I + \psi_U + 2\omega t)) \quad (2.8)$$

$$= I_{rms} U_{rms} (\cos(\psi_I - \psi_U) - \cos(\psi_I + \psi_U + 2\omega t)) \quad (2.9)$$

¹We will use the letter u to describe the instantaneous value of the voltage, which comes from the German word "Unterschied", meaning difference, and a voltage is, in fact, a potential difference.

As we see here, multiplying sine waves with different phases and magnitudes becomes complicated. We are only interested in the magnitude and phase of the sine wave, so we can draw a parallel to the complex field, in which we represent a number by its magnitude and phase. In that case, the complex current is given by:

$$i(t) = \hat{i}(\cos(2\pi ft + \psi_I) + i \sin(2\pi ft + \psi_I)) \quad (2.10)$$

$$= \hat{i}e^{i(\omega t + \psi_I)} \quad (2.11)$$

and similarly for the voltage:

$$u(t) = \hat{u}(\cos(2\pi ft + \psi_U) + i \sin(2\pi ft + \psi_U)) \quad (2.12)$$

$$= \hat{u}e^{i(\omega t + \psi_U)} \quad (2.13)$$

Another important aspect of our electricity grid is that most transmission happens in three phases, so each wire has a current with a different phase. The main reason for using three phases instead of one is the following. A single-phase 220V circuit with 6A wiring can deliver $220 \cdot 6 = 1320VA$, where VA is the unit of the apparent power ($1VA \approx 1W$). On the other hand, a three-phase 220V circuit with 6A wiring can deliver $3 \cdot 220 \cdot 6 = 3960VA$, which is 300% more than a single-phase circuit, but with only 67% more wiring. To obtain the phase difference between phases, we need to divide the period (2π) by 3. Then similarly to Figure 2.1, we can write the three-phase current by three sinusoidal functions as in Figure 2.2 and the following equations:

$$i_1(t) = \hat{i} \sin(2\pi ft + \psi_I) \quad (2.14)$$

$$i_2(t) = \hat{i} \sin(2\pi ft + \psi_I - \frac{2}{3}\pi) \quad (2.15)$$

$$i_3(t) = \hat{i} \sin(2\pi ft + \psi_I + \frac{2}{3}\pi) \quad (2.16)$$

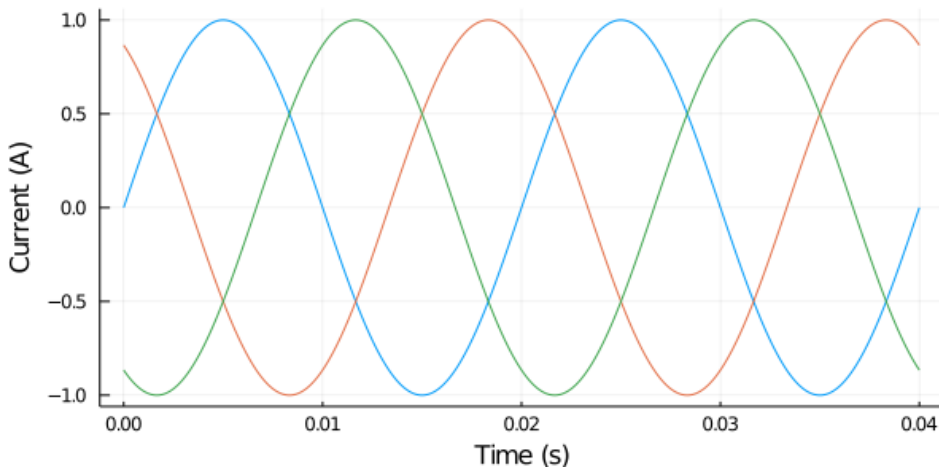


Figure 2.2: A three-phase sinusoidal curve at 50Hz

and their complex counterpart:

$$i_1(t) = \hat{i}e^{i(\omega t + \psi_I)} \quad (2.17)$$

$$i_2(t) = \hat{i}e^{i(\omega t + \psi_I - \frac{2}{3}\pi)} \quad (2.18)$$

$$i_3(t) = \hat{i}e^{i(\omega t + \psi_I + \frac{2}{3}\pi)} \quad (2.19)$$

At this point, we have covered the essential mathematical aspects of the electricity grid for this research. The following section will discuss what components a distribution network has, and the section after that zooms in onto transformers.

2.2. Components in a distribution network

Drawing the electric distribution system schematically results in Figure 2.3. On top, we have the high power producing power plants, which in the Netherlands are mainly coal and gas-powered, but also the nuclear reactor in Borssele falls in this category. Big overhead powerlines then transport this electricity over long distances. The Transmission System Operator (TSO), which in the Netherlands is TenneT, manages these cables. These power lines end at big industrial consumers and in large power transformers. Companies like Stedin, called Distribution Network Operators (DNOs), manage these power transformers and everything between these transformers and our homes. In the figure, the two overlapping circles are the locations where transformers are present.

From these power transformers, the electricity is transported through underground cables to the smaller distribution transformers [13]. The electricity goes through switchgear before the wires enter the power and distribution transformers. If service technicians need to perform maintenance at the transformer, the transformer needs to be de-energized to prevent the service technician from getting electrocuted. Switch gears completely turn off the electricity coming into the transformer, making it safe for the service engineer to perform maintenance.

Another component where electricity is passing through is a circuit breaker. Circuit breakers work in situations where a high current suddenly comes through. If this high current enters the transformer, it would energize too much and permanently damage it. A circuit breaker acts as a sort of switch: when the current is too high, it creates a strong magnetic force that switches a lever, breaking the current and thus stopping the flow of electricity.

Similar to a circuit breaker, the power also passes through fuses. A fuse is a thin wire that breaks at a specific voltage to prevent the high voltage from passing through and damaging materials further down the grid. Fuses are also used in everyone's home to prevent a high voltage from passing through the wall outlets.

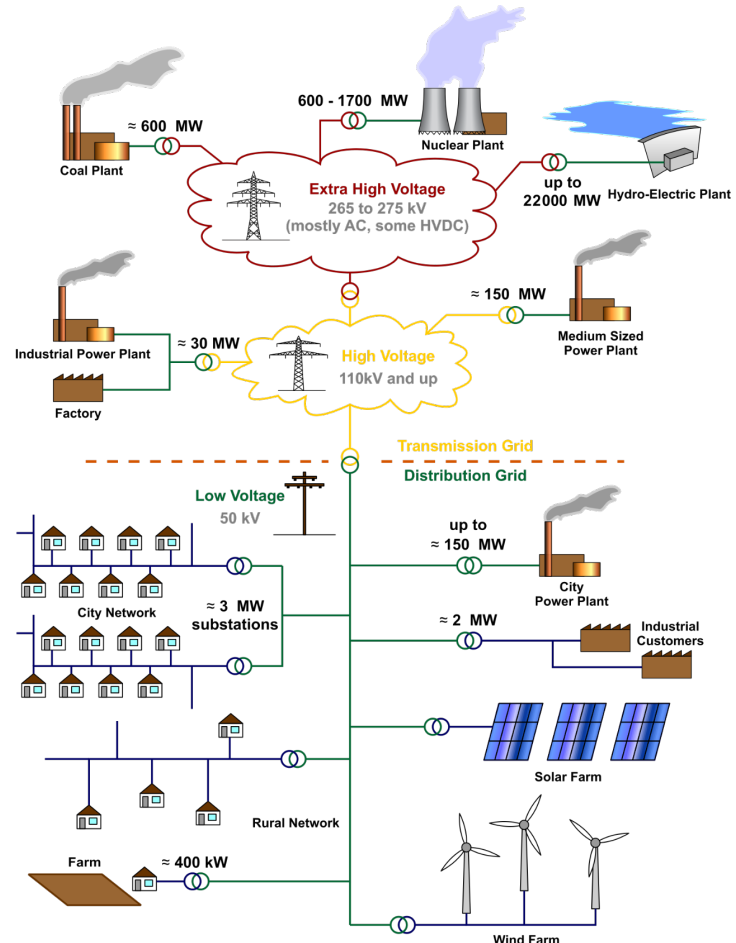


Figure 2.3: A high-level view of an electricity network [14]

2.3. Types of transformers

Worldwide there are many types of transformers, from the charger for a phone to big power transformers outside like the one shown in Figure 2.4. Since we conducted this research at network operator Stedin, we are only interested in the transformers needed to transport electricity from one place to another. Stedin divides these transformers into two categories: power and distribution transformers, where the main difference between them is their power rating [15]. Power transformers have a rating of more than 10 MVA, whereas distribution transformers have a rating of 1 MVA or less. Most Stedin distribution transformers have a capacity of 400 or 630 kVA, which can supply approximately 120 and 190 households, respectively, if no high power equipment such as heat pumps are installed [13].



Figure 2.4: In service power transformer [16]



Figure 2.5: Distribution transformer [17]

2.4. Workings

Transformers work because of the principles derived by Faraday in the 19th century, where he let an alternating current through a copper wire wound around an iron core. In this research, we will call this wire a winding. First, he observed that this setup generated a magnetic field inside the core. Next, by winding another wire around the core, this magnetic field induced a current in the other winding. Then by varying the number of windings on each side, he could create a current with more or less ampere than what he started with.

When looking at a single winding, the magnetic flux through that loop is equal to [12]:

$$\Phi = \iint \mathbf{B} \cdot d\mathbf{A} \quad (2.20)$$

Where Φ is the magnetic flux, \mathbf{B} is the magnetic field, and \mathbf{A} is the area enclosed by the winding. Then Faraday's law of induction states that the induced voltage is equal to the rate of change of the magnetic flux:

$$V_{in} = \frac{d\Phi}{dt} \quad (2.21)$$

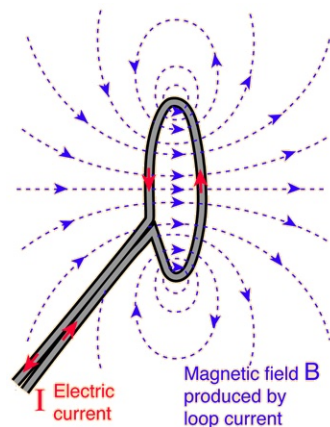


Figure 2.6: Single coil with a current passing through, inducing a magnetic flux according to the right-hand rule [18].

With this equation, we also see why we need an alternating current: with a direct current, the rate of change of the magnetic flux would be 0 as the magnetic field would remain the same, and thus no voltage will be induced.

The last two equations work both ways: when we apply an alternating current to the coil, this induces an alternating magnetic flux inside the area enclosed by the loop. When another coil is around this magnetic flux, it induces a current in the coil. A current will flow if we connect the second coil to a terminal.

Up to this point, we only looked at a single-coil, but by having multiple coils, one can increase the induced voltage with the same magnetic flux since:

$$V_{in} = N \frac{d\Phi}{dt} \quad (2.22)$$

Where N is the number of turns. If the conversion mentioned in the previous paragraph is perfect, the voltage induced by one winding will equal the voltage in the other winding. Now, if these windings have a different number of turns, we can increase or decrease the induced voltage in the second winding, since:

$$\left. \begin{aligned} \frac{d}{dt} \Phi_1 &= \frac{V_{ind,1}}{N_1} \\ \frac{d}{dt} \Phi_2 &= \frac{V_{ind,2}}{N_2} \\ \Phi &= \Phi_1 = \Phi_2 \end{aligned} \right\} \frac{d}{dt} \Phi = \frac{V_{ind,1}}{N_1} = \frac{V_{ind,2}}{N_2} \Rightarrow \frac{V_{ind,1}}{V_{ind,2}} = \frac{N_1}{N_2} \quad (2.23)$$

If we then assume that the power applied to the first coil is equal to the power received by the second coil, we get for the current:

$$\frac{N_1}{N_2} = \frac{V_1}{V_2} = \frac{\frac{P}{I_1}}{\frac{P}{I_2}} = \frac{I_2}{I_1} \quad (2.24)$$

So an increase in voltage is paired with a decrease in current. This relation is also why transformers are so essential to our electricity grid. We want to transport the electricity with the smallest current possible as this will generate the lowest amount of power loss, which is given by $P_{loss} = I^2 R$, where R is the resistance of the wire transporting the current.

2.5. Components

A transformer is a complicated piece of equipment with multiple components. Therefore, we will only discuss the most important ones for this research here. In Figure 2.7, one can see the inner parts of a transformer. Part of the information in this section comes from a visit to transformer manufacturer IEO.

Core

Transformer manufacturers make the core of a transformer out of very thin slices of silicon steel. They use steel since it can transport the magnetic field easier than air. This process is physically described by the magnetic permeability (μ), which is three orders greater for steel than for air (1500 vs 1) and is thus better at conducting the magnetic flux. Manufacturers use thin slices of steel, also called laminations, to maximize the flux going through the core and minimize the losses. These thin slices are around 0.5 mm thick, and manufacturers stack



Figure 2.7: This figure shows the inside components of a transformer. The grey part is the transformer's core, through which the magnetic flux passes. The brown parts are the windings encircled with paper for better insulation. There are holes in the paper to have oil circulating more closely around the windings [19].

them on top of one another with a layer of varnish in between to prevent the flux from going in all directions [20].

There are multiple configurations possible for a three-phase transformer core, but manufacturers usually choose one of two possibilities: a core type or a shell type, as given in Figure 2.8.

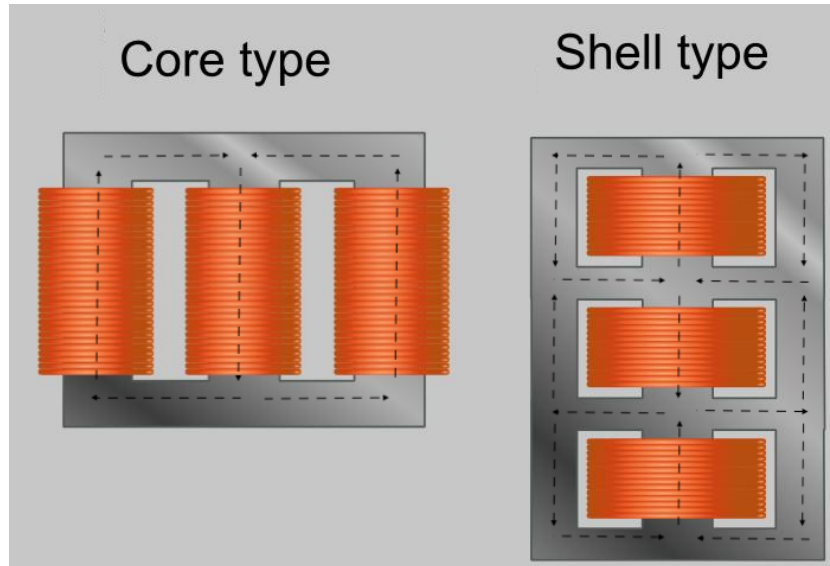


Figure 2.8: Two types of transformer configurations, where the arrows indicate the flow of magnetic flux (modified from [21])

The arrows in the figure represent the magnetic flux, which alternates in direction due to the alternating current passing through the windings. For the shell type, we see that each winding has its magnetic flux path, and thus each phase of the current is more independent, making it more suitable for a place with a constant unbalanced load. However, since most of the time, the load is balanced, the core type transformer is most commonly used.

Winding

As we said at the end of Section 2.1, our electricity is transported in three phases, so we need one wire for each phase and one set of windings per phase in a transformer. One can see these windings in Figure 2.7, where we see three cylindrical shapes around a core, with closest to the core the secondary winding encapsulated by the primary winding. Manufacturers place the secondary winding closest to the core to have the flux travel the shortest distance and thus minimize the flux loss to the surroundings. The windings are often made from copper or aluminium as these have a high electrical conductivity ($\sigma = \mathcal{O}(10^7) \text{ S/m}$). In contrast, air has a conductivity of $\sigma = \mathcal{O}(1) \text{ S/m}$, where the conductivity is a measure of how easy the material can transport electricity.

In most schematic drawings online, we see that both windings are circular copper wires. Historically, this was the case, but nowadays, the windings are different. Most of the time, manufacturers use aluminium since it is cheaper to manufacture and has a conductivity in the same order of magnitude as copper [22]. Also, very thin sheets of aluminium, called foils, are used for the secondary winding. These foils have a relatively large cross-sectional area, increasing the amount of current flowing through them [23]. We will return to this fact later on.

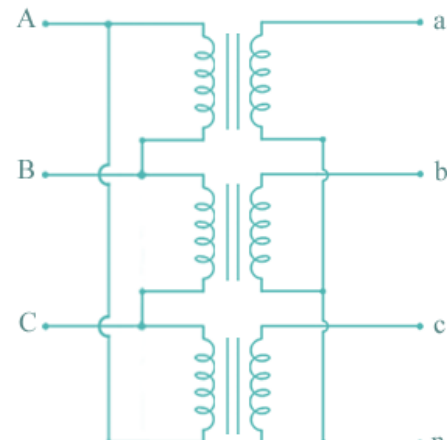
Connection

We have three wires entering the transformer at the three brown pillars at the back of Figure 2.5. To ensure that a balanced load reaches the transformer, these wires are connected to one another before connecting to the windings. The most common way is with a delta or a wye connection. The names come from the way the connections look like if you lay them flat on the ground: with a delta connection, it will look like a triangle, each winding is connected with the one after it, and with a wye connection, it will look like a Y, with all windings connected to a central point. Most distribution transformers have a delta-wye connection, so a delta connection on the high voltage side and a wye connection on the low voltage side, as illustrated in Figure 2.9 [20].

There are numerous advantages to having the windings connected like this. For a delta connection, this is reliability: if one of the windings fails, the other two can still produce the same voltage, whereas if a winding fails in the wye connection, this will result in a reduced voltage. There is a wye connection on the secondary to counteract unbalanced loads, as the central point is often grounded. This grounded wire causes the excess current in an unbalanced load to move into that neutral wire and is therefore not distributed over the rest of the grid.

Insulation

Looking back at Figure 2.7, we cannot see the windings. This is because there is insulation material around the windings to prevent the core from coming into contact with the windings and the windings from coming into contact with one another. The insulation material used here



$\Delta - Y$

Figure 2.9: Schematic drawing of a delta-wye connection in a three-phase transformer. We see the three high voltage cables entering the transformer on the left. These are connected in a triangular shape: the end of wire A is connected to the beginning of wire B, the end of wire B is connected to the beginning of wire C, and the end of wire C is connected to the beginning of wire A. On the right, we can see a wye connection, where the end of each low voltage wire is connected to the neutral wire, given by n [24].

is an oil-impregnated solid pressboard. This material has high dielectric strength, meaning that it can withstand current passing through, and it can withstand high temperatures very well. The oil-impregnated part is important: the solid pressboard has tiny air gaps, reducing the insulating strength and the amount of heat the paper can dissipate [25]. So the pressboard is filled with oil before placing it in to prevent the oil inside the transformer to fill those air gaps.

Tank

Manufacturers place the core, windings, and insulation material inside a steel tank. This tank protects the core and windings from the external environment and holds the cooling material.

Tank filling

There are two types of cooling mechanisms for transformers: oil-filled or air-filled.

Oil-filled transformers

For oil-filled transformers, the core and windings are placed in a tank together with transformer oil. The oil provides added insulation, better heat dissipation, and fault detection features. There are a couple of factors important for oil: moisture, acidity, breakdown voltage, and furans. In large power transformers, a service technician can take a sample of the oil, and a laboratory can perform an oil analysis to establish the concentration of each of these factors [15].

Dry type transformers



Figure 2.10: The main parts of a dry-type transformer which are placed inside a sealed tank [26].

We cannot fill all transformers with oil. Since oil is a flammable product and a fire can cause severe damage to the environment, it is forbidden to place oil-filled tanks in certain places, such as in high apartment buildings or national parks. Therefore, we need transformers with different insulation materials to power those areas. As an insulation material, often, epoxy resin is chosen as this material can withstand heat and protects the windings and core from coming into contact with moisture and other pollutants. The windings, core, and epoxy resin are placed inside a sealed tank, which often looks different from an oil-filled transformer because it needs more air for ventilation.

The ageing process in dry-type transformers is modelled differently than that in oil-filled transformers, and for this study, we will only consider the oil-filled transformers.

Cooling

The process of having current at one voltage going through a wire, transforming into a magnetic flux, transforming into a current with a different voltage through a wire is not perfect. At multiple points in this process, losses occur. We will explain these losses further in detail in Section 3.1, but for now, we only care about the fact that these losses cause heating. This heating causes the paper to deteriorate, and the higher the temperature, the faster the deterioration process goes. When this process has reached a point where one winding comes into contact with another winding or the core, it will cause a short circuit, and the transformer will break down. It is vital not to let the oil temperature rise too much to prevent this from happening. Manufacturers do this by placing reinforcement ribs on the sides of the transformer. These ribs are thin and therefore have a large surface area, but only a small volume where the oil fits in. This means that the tank has a larger area exposed to its surroundings, giving more cooling capabilities to the oil. In Figure 2.5 the cooling ribs are the thin vertical extensions to the rectangular transformer tank.

In most distribution transformers, this cooling process happens naturally: the heat produced in the oil around the core and windings moves to the top of the transformer. From there, it moves along the sides where the cooling ribs are to cool it down even more and eventually reaches the bottom where it starts to heat up again by the core and windings. However, we want this cooling process to happen faster for larger transformers, as the core and windings produce more heat. Therefore, manufacturers can do multiple things to accelerate the cooling process: larger and more cooling fins, choosing an oil type with a higher heat conductivity, or forced cooling. With forced cooling, the cooling process works like an inverted radiator: some of the hot oil moves from the top of a transformer into a breathing tank, where it cools down and then flows back into the lower part of a transformer. Figure 2.4 shows a transformer with a breathing tank, namely the horizontal cylinder at the back of the transformer. These tanks are present in all power transformers and some of the older distribution transformers. Different mnemonics exist for the different types of cooling: ONAN (where the air and oil flow naturally), ONAF (where the oil flows naturally through the transformer, but the air flows strong around the transformer using ventilators to speed up the cooling process), and OFAF (both oil and air are forced through or around the transformer), where the last one has the best cooling mechanism but is also the most expensive to build. For example, in Figure 2.4, we see some fans on the cooling ribs, so this could be an ONAF or an OFAF transformer.

As distribution transformers in the Netherlands are often located in very narrow spaces, like the ones in Figure 2.11, it is also essential to have good ventilation systems in these spaces, but we will not consider the different ways to do this and how to model this.

Other components in a transformer

At this point, we have mentioned and discussed the most critical components of a transformer for this research. We will shortly discuss the other components below.



Figure 2.11: Different stations where distribution transformers are in.

The high voltage cables connect with the transformer at the three high pins we see in Figure 2.4. In Figure 2.5, these are the three brown cylindrical shapes at the back, with one being behind a thermometer. These are called bushings, and they are often made out of porcelain to prevent the current from coming into contact with the transformer tank [20].

Another part of the transformer is the load tap changer. When building a transformer, the manufacturer can determine the winding ratio. So if we, for example, want to convert $10kV$ to $220kV$, we use Equation 2.24 and see that we need 45 times more windings on the primary side than on the secondary side. If we would then have a current of $15A$ on the primary side, this results in $681.8A$ on the secondary side, generating $15kW$ of power. What if the consumer needs more power for a short amount of time? Building a new transformer with a different winding ratio would be a waste of money because the consumer only needs this extra power for a short period. To meet the demand, transformer manufacturers came up with the tap changer. We can change the number of windings in each coil with this tap changer [20]. So a transformer manufacturer will build a transformer with a ratio of 50:1 but will only use 45:1 as a standard. However, this tap changer is rarely used for distribution transformers as consumers often need more power for a more extended period of time. At that point, Stedin places a transformer with a higher capacity.

Lastly, there is the oil tank. The oil tank is visible at the back of the power transformer in Figure 2.4 as a horizontal cylindrical shape. An oil tank is present in all power transformers and some of the older distribution transformers. With an oil tank, the warm oil flows out of the transformer into the oil tank, where it is more exposed to the outside air. Then when this oil cools down, it goes back into the transformer. This process repeats itself, circulating the oil around to keep cooling the core and windings of the transformer.

2.6. Harmonics

The last component to discuss is harmonics. Typically, our alternating current behaves as a sinusoidal wave, as in Figure 2.1. However, this sine wave gets distorted with the rise of electronics, such as LED lights and computers, which all draw power immediately [27]. Another source of distortions in the sine wave is non-linear loads. Non-linear loads do not have a sinusoidal current but have a pulse current or are discontinuous. With the increase of these different loads, the sinusoidal curve we would typically have gets distorted. In most cases, this distortion is only small, but in neighbourhoods where there are a lot of solar panels and electric cars, these effects add up and can cause a significant change in the way the current curve looks.

If we visualize this, the current would typically look like the blue curve in Figure 2.12. However,

with the increase of non-linear and unbalanced loads, this curve changes into the orange curve in the same figure. Previously, our current could be described by a pure sinusoidal function, like the one in Equation 2.1. To mathematically describe this newly created function, we can use Fourier series. A Fourier series is a weighted sum of sinusoidal functions, given by Equation 2.25.

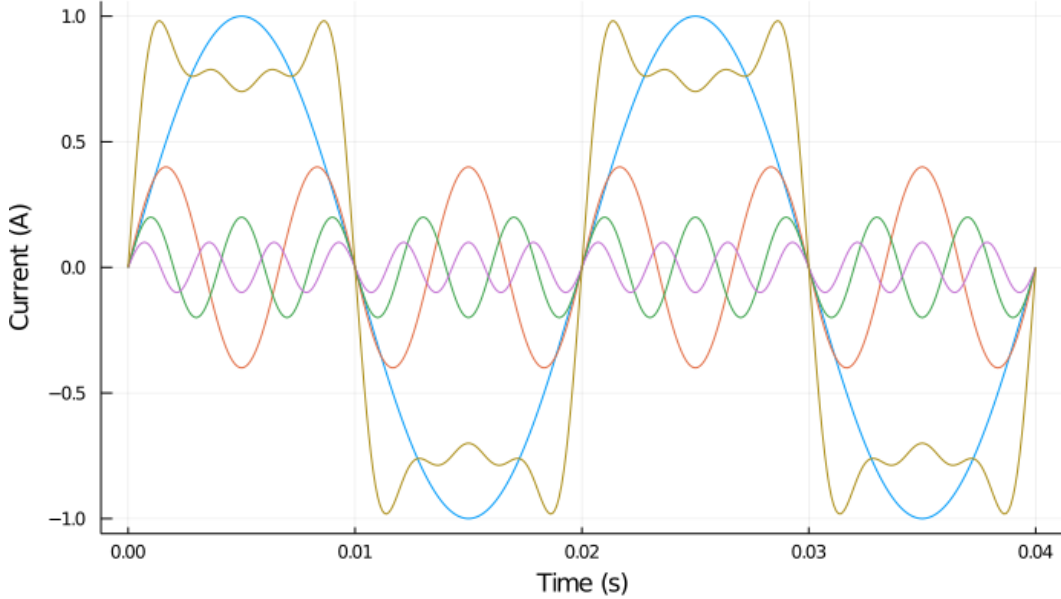


Figure 2.12: This figure shows the distortion in the current due to the influence of harmonics in the network

$$I(t) = \sum_{n=1}^N [\hat{i}_n \cdot \sin(n\omega t)] \quad (2.25)$$

The following Fourier series describes the orange curve, where $\omega = 2\pi f$:

$$I(t) = \sin(\omega t) + 0.4 \sin(3\omega t) + 0.2 \sin(5\omega t) + 0.1 \sin(7\omega t) \quad (2.26)$$

The total harmonic distortion (THD) is a simple way to indicate how many harmonics are in the system without calculating each current individually every time. It is given by:

$$THD_I = \sqrt{\sum_{n=2}^N \left(\frac{I_n}{I_1}\right)^2} \cdot 100\% \quad (2.27)$$

In the case of Figure 2.12 , the THD is equal to:

$$THD_I = \sqrt{\frac{0.4^2 + 0.2^2 + 0.1^2}{1}} \cdot 100\% = 45.8\% \quad (2.28)$$

With this value, organizations have set norms to indicate what percentage of harmonics is safe in the electricity network for a given timeframe. For example, this norm states that for 95% of the time, the THD for $N = 40$ should be lower than 8%, and for 99.9% of the time, the THD should be below 12% [13].

The most important effect of having harmonics in the electrical circuit is extra heat. This excess heat occurs in the cables transporting the electricity and in transformers. Multiple parts of a transformer will become warmer: the windings, the neutral wire at the secondary side and the core itself. All this extra heat causes the insulation material to deteriorate faster, thus reducing the transformer's lifespan.

2.7. Current asset management

As a final part of the introduction to the electricity grid, we will shortly discuss what Stedin currently does for asset management for distribution transformers. The short answer is that there is little to no maintenance for distribution transformers, as it is unnecessary. Instead, a service technician visits their location every 3-8 years after installing a transformer. During a visit, the service technician checks if there is oil leaking from the transformer, which would indicate a hole in the tank, determines if it is not extremely warm in the room around the transformer and checks the drag indicator ("sleepwijzer" in Dutch). The drag indicator gives the maximum current since the technician last entered the room. Unfortunately, this indicator only shows one maximum value, so we do not know if we had 95% of this current for a more extended period or only shortly when a short circuit occurred. This did not matter until now because the load was predictable, with a peak in the morning when people wake up and a peak in the evening when people come home, turn on the radiator, and watch TV. However, with the transition to more variable loading patterns due to decentralized power generation on roofs, this structure in asset management will not be sufficient.

More maintenance is being done for larger power transformers, as these are more expensive and time-consuming to replace, and therefore Stedin needs to know when one might fail. In this case, the service technician checks the same things as for distribution transformers but can also perform a dissolved gas analysis. The service technician taps a bit of oil from the transformer and sends it to a laboratory to perform such an analysis. In the laboratory, they test the oil for the amount of moisture, acids and furans. Furans are a product of the breaking down process of the paper insulation material. A high percentage of furans in the oil implies that a lot of paper has broken down, i.e., the transformer is near the end of its lifetime. This analysis is often impossible for distribution transformers since most distribution transformers do not have a tap on the oil tank from which we can take a sample.

3

The behaviour of a transformer

To make a model of the remaining life of a transformer, we need two things: the components in a transformer, as mentioned in Section 2.5, and the way these components behave in regular operation. Furthermore, as mentioned in that same section, the transformation from one voltage to another is imperfect, and losses occur. This chapter describes the different types of losses for a transformer, followed by their effect, mainly heat. Lastly, we describe the other physical aspects of a transformer.

3.1. Losses

In the ideal world, the voltage passing through a transformer would be transformed into a lower voltage by precisely the ratio of the windings, as discussed in Section 2.4. However, we don't live in an ideal world. Since the transformer does not have any moving parts which can deteriorate, there are almost no mechanical losses. However, there are multiple electrical losses. Usually, we categorize these losses into two categories: load and no-load losses [15]. As the name suggests, load losses are the losses that depend on the load, and the no-load losses are the losses that are always present, no matter the variation of the load. However, the effects of harmonics, which are load-dependent, occur in the phenomena described by no-load losses. Hence, we will categorize the losses in this section per component in the transformer instead of load and no-load losses.

Core losses

The core or iron losses are the losses that occur in the core of the transformer. We can divide these into two types: hysteresis and eddy current loss. Most times, both these losses are considered no-load losses. However, when calculating them, they are both dependent on the frequency, meaning that when considering harmonics, which are sums of higher frequencies, these losses suddenly become load losses.

Hysteresis loss

As mentioned before, the transformer's core is made out of thin silicon steel sheets. When the molecules in this steel are excited by a magnetic field, they are oriented in the direction of this field. However, the magnetic field changes at a rate of 50 times per second (since the current frequency is 50 Hz), so the molecules also change their direction 50 times a second. The molecules cannot keep up with changing direction so rapidly, and thus losses occur. These losses are called hysteresis losses [28].

We describe this phenomenon with a B-H curve, as illustrated in Figure 3.1. When steel manufacturers produce their steel, the curve starts in the centre. After fabrication, the material is susceptible to a magnetic field intensity H . Imagine this material being a sponge and the magnetic field intensity the water. A sponge can only absorb a maximum amount of water until it is full, and magnetic materials have the same behaviour. When a certain maximum flux density is reached, B_{sat} , the material goes into saturation and is unable to absorb any more magnetic field. If we lower the field intensity and change its direction (which happens with an alternating current), the flux density also reduces. However, this process is not linear, as illustrated with the left-most line in the figure. When the material reaches its minimum flux density, $-B_{sat}$ in the figure, again saturation occurs, and the process repeats itself.

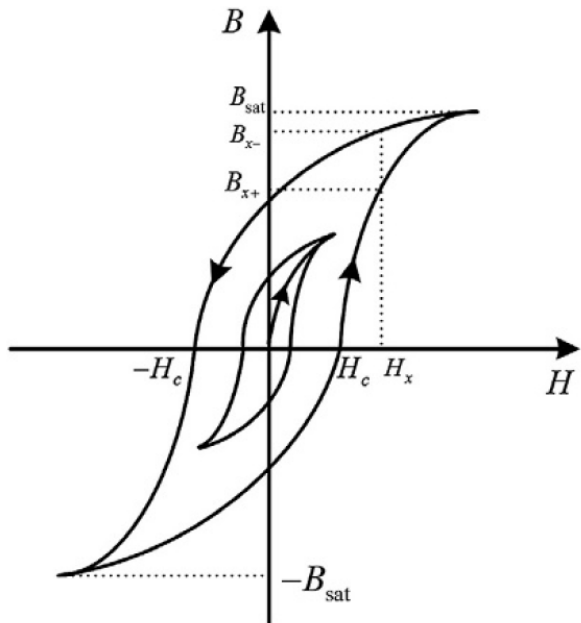


Figure 3.1: B-H loops of a magnetic material [29]

The area enclosed by this loop is the hysteresis loss of the material. Transformer manufacturers can reduce hysteresis loss by using grain-oriented steel. This steel has a narrower magnetization curve and a higher point of saturation, B_{sat} .

Eddy current loss

Because of Faraday's law of induction, the magnetic field that induces a current in the windings also induces a current inside the core. This current flows in loops, as illustrated in the left figure of Figure 3.2, where a magnetic field B travels through a homogeneous block of iron. Bigger loops of current in the core mean less current in the windings.

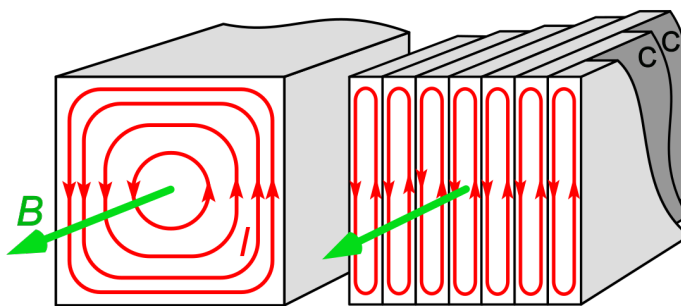


Figure 3.2: Magnetic field travelling through a solid and laminated block of steel [30]

To minimize the effect of these loops of current, also called eddy currents, the core is divided into tiny sheets, as illustrated in the right figure of Figure 3.2. Then, manufacturers place a non-conductive coating between each sheet, so almost no current can pass between the laminations. This means that the created loops of current are a lot smaller in area, and since the magnitude of the current is proportional to the area enclosed by the loop, the resulting current will be a lot smaller, so fewer losses occur [20].

The hysteresis loss is most important for lower frequencies, whereas the eddy current loss becomes dominant at higher frequencies [31].

Winding losses

Winding loss, often also called copper loss, is the loss in the windings. When having a wire, the power at the beginning is not the same as the power in the end. Mathematically, the loss for a wire is $P_{loss} = I^2 R$, where R is the resistance of the wire. Manufacturers can minimize the copper loss by using materials with a large cross-sectional area and high electrical conductivity to reduce the resistance.

There are two other losses in the windings when higher frequency currents are present: the skin and proximity effects. These effects alter the current distribution when looking at a cross-section for the windings at higher frequencies. However, as the windings are small in diameter, these effects are negligible.

Other losses

Not all electric current inside the primary winding converts to magnetic flux inside the core. The current also induces a flux in the clamps supporting the core and windings, the bolt supporting these clamps, and the tank surrounding the core. These losses are stray losses, which can be considered negligible [32].

3.2. Physics inside a transformer

In the previous section, we described the losses coming from the electromagnetic behaviour. However, besides electromagnetic behaviour, there are more physical behaviours. These are illustrated in Figure 3.3. The following section describes the right part of the figure, the physics of heat transfer and the effect of oil flow, which one can model with computational fluid dynamics (CFD). After that, we describe the left part of the figure, so the solid mechanics in a transformer.

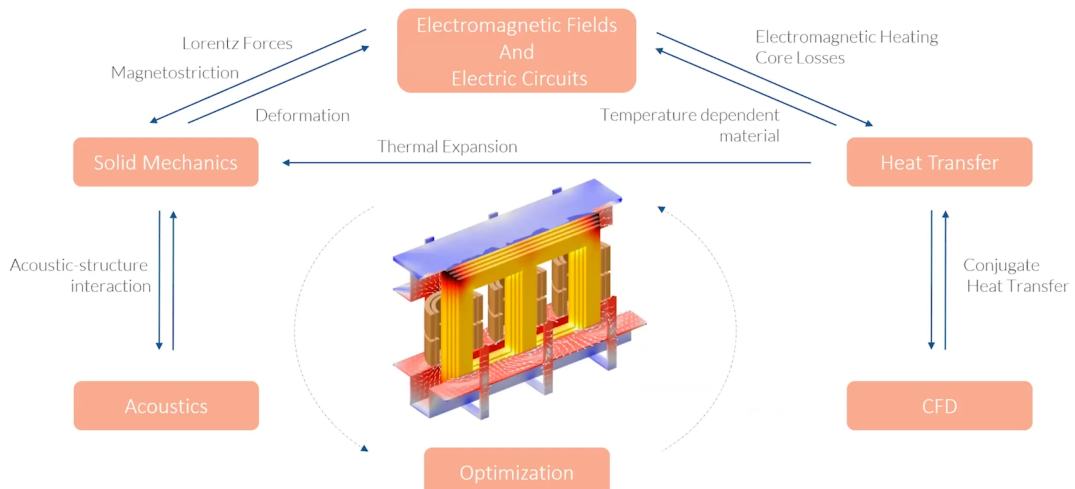


Figure 3.3: Multi-physical behaviour of a transformer [33]

3.2.1. Heat

The hysteresis and eddy current loss cause heat in the core, the I^2R loss causes the windings to heat up, and the stray losses cause the tank to heat up. Manufacturers place oil in the transformer to transport this heat. The heat disperses towards the side with the oil, where cooling ribs cool down the oil even more.

However, the oil can not quickly disperse all the heat, so the core and windings will remain warm. In addition, the heat can cause multiple problems for the core and windings, such as reduced mechanical strength of conductors, insulation materials and the carpentry supporting the transformer, reduced electrical conductivity of the windings, and, most importantly, a breakdown of the paper insulation surrounding the windings. This breakdown then causes tiny pieces of paper to get stuck in the fins surrounding the transformer, making it harder for the oil to cool down causing even more paper to degrade. Another problem with the broken-down paper insulation is that the windings can come into contact with one another at some point, causing a short circuit that could set the oil and thus the whole transformer on fire.

The amount of paper that has broken down is a measure of the remaining life of a transformer. This is called the degree of polymerization (DP) value [34]. The DP value is between 1100 and 1400 when the transformer is built. This value first slowly, and at the end of its lifetime, rapidly decreases to 0. A service technician can measure the DP value by taking an oil sample. However, since Stedin does not take oil samples from distribution transformers, models need to be made about the temperature.

3.2.2. Solid mechanics

When the temperature increases, this also affects the materials inside a transformer. For instance, the conductivity of the windings decreases when the temperature increases, creating a higher resistance and thus more losses inside the transformer. Also, as mentioned before, higher temperatures cause the paper to break down, leading to a reduced life span.

Another aspect of the behaviour of transformers is their vibration. This is caused by the alternating current making the materials in the transformer vibrate. When a short circuit occurs in the transformer or the paper is too far degraded, the vibrations of the transformer will be different. We can measure the difference in vibration when taking the transformer from the grid [35].

At this point, we discussed the components in a transformer, their general behaviour and the consequences of that behaviour on the condition of the transformer. With all these tools at hand, we can make a first model to determine the loss of life under a certain load with the loading guide.

4

The loading guide

The loading guide is the first step to determine the remaining life of a transformer without knowing much about it. It was formalized into norms in 1981 to simplify calculating what a particular load profile did to the remaining life [36]. As mentioned previously, we can determine the remaining life by measuring how much paper has degraded. However, modelling the paper degradation is very difficult, as there are multiple processes in play: oxidation, hydrolysis and pyrolysis [34]. Hence, the idea behind the loading guide is that the leading cause of reduction in the lifetime of a transformer is the temperature, as a high temperature causes the paper to break down faster. The temperature distribution has to deal with all kinds of non-linearities and fluid flow models, so for a simple approximation, one temperature value is chosen: the hot spot temperature. A time series of this temperature value then determines the percentage of life loss.

The loading guide chooses the hot spot temperature as an arbitrary point in the transformer, representing the warmest point. This point is somewhere on top of the windings, close to the core, but in reality, each transformer has a different hot spot, which also changes under various loads. Also, the name is slightly misleading as the hot spot temperature used in the loading guide is not the warmest point in the transformer but one fixed point a certain distance away from the top.

The loading guide is based on the schematic drawing in Figure 4.1. This figure shows the temperature distribution inside a transformer tank. The loading guide assumes that the oil temperature rises linearly from bottom to top, as illustrated with the diagonal lines in the picture [34]. The line on the left represents the temperature outside the windings, and the line on the right the temperature inside the windings. This figure shows that the loading guide also assumes that the temperature changes linearly from outside to inside the windings. Additionally, we see that the hot spot temperature is a factor H higher than the temperature at the top of the winding.

The loading guide is the current standard for transformer operators to determine its loss of life under a particular load [37], [38]. Even though it is simple, according to a CIGRE review, where they compared the loading guide results with measurements using optical probes, the loading guide gives very accurate results [39], [40].

We will introduce and discuss the two versions of the loading guide: the IEEE loading guide [41] and the IEC loading guide [34]. In the end, we will discuss the addition of the influence of harmonics to the loading guide. But first, we give the calculations to determine the loss of life from the hot spot temperature.

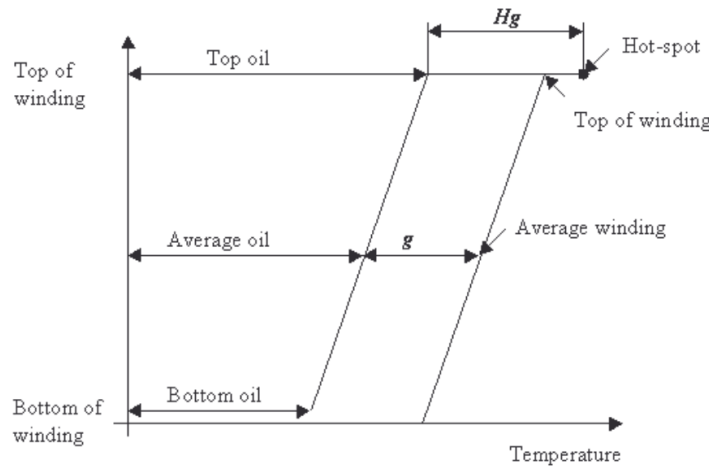


Figure 4.1: Basic thermal diagram used in the loading guide [42].

4.1. Transformer life loss calculation

Both loading guides first present how the lifetime of a transformer reduces, which happens by the high temperatures breaking down the paper insulation. As mentioned before, both guides consider a hot spot temperature, and the equations for loss of life are based on this variable. Both guides make a distinction between thermally upgraded paper and non-thermally upgraded paper. Manufacturers developed the thermally upgraded paper in the 1950s, and this paper is better able to withstand heat and will thus have a longer lifetime [43]. As seen in Figure 1.1, Stedin still has some transformers from before 1960. Therefore, if Stedin wants to use the loading guide to determine the loss of life for these transformers, the following equation has to be used:

$$F_{AA} = 2^{(\theta_h - 98)/6} \quad (4.1)$$

Where θ_h is the hot spot temperature.

This equation uses a reference temperature of 98°C , so when the temperature rises to more than that, the transformer will age faster than was set by the manufacturer.

The equation for the thermally upgraded paper is based on the Arrhenius equation and is given by:

$$F_{AA} = A \exp\left(\frac{B}{\theta_h + 273}\right) = \exp\left(\frac{15000}{110 + 273}\right) \exp\left(-\frac{15000}{\theta_h + 273}\right) \quad (4.2)$$

The loading guide uses a reference temperature of 110°C for thermally upgraded paper.

Comparing the two side by side gives Figure 4.2, where the ageing acceleration factor on the y-axis is on a log scale.

The equation for F_{AA} gives the ageing factor for one data point. Then, to compare the ageing over time, the equivalent ageing factor is introduced:

$$F_{EQA} = \frac{\sum_{n=1}^N F_{AA,n} \Delta t_n}{\sum_{n=1}^N \Delta t_n} \quad (4.3)$$

Here $F_{AA,n}$ is the ageing acceleration factor at time interval n , Δt_n is the length of the time interval, and N is the number of time intervals.

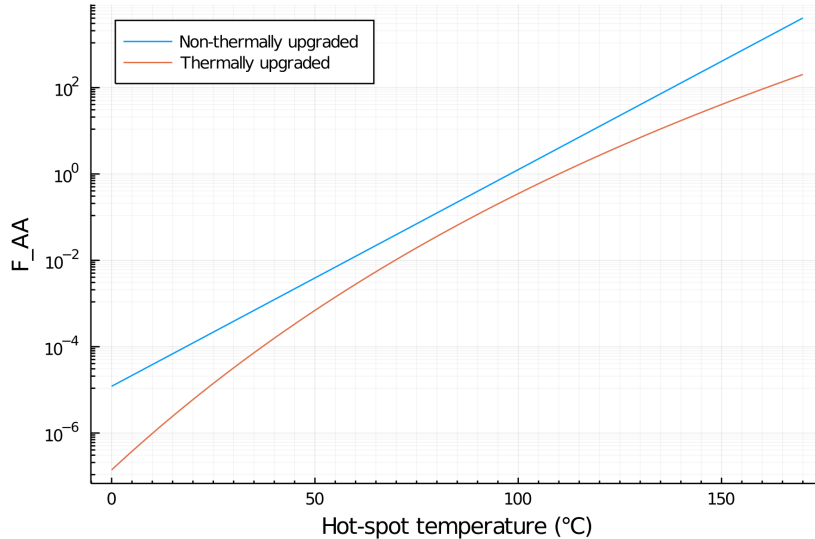


Figure 4.2: Comparison between ageing acceleration factor of non-thermally and thermally upgraded paper

We can then use this equation to calculate the percentage loss of life over a time period t :

$$\% \text{Loss of Life} = \frac{F_{EQA} \cdot t \cdot 100\%}{\text{Normal insulation life}} \quad (4.4)$$

According to [44], the transformer should work at rated load for at least 180.000 hours = 20.5 years, so we can set this number as normal insulation life.

4.2. IEEE loading guide

In the IEEE loading guide [41], the hot spot temperature consists of a sum of three components:

$$\theta_h(t) = \theta_A + \Delta\theta_{TO}(t) + \Delta\theta_H(t) \quad (4.5)$$

Where θ_A is the average ambient temperature during the studied load cycle, $\Delta\theta_{TO}$ is the top oil rise over ambient temperature, and $\Delta\theta_H$ is the hot spot to top oil temperature rise. The top oil temperature is the sum of the first two terms in the equation.

The second term is calculated from the following equation:

$$\Delta\theta_{TO}(t) = (\Delta\theta_{TO,U} - \Delta\theta_{TO,i}) \left(1 - \exp \left(-\frac{t}{\tau_{TO}} \right) \right) + \Delta\theta_{TO,i} \quad (4.6)$$

with parameters:

$$\Delta\theta_{TO,i} = \Delta\theta_{TO,R} \left(\frac{1 + RK_i^2}{1 + R} \right)^n \quad (4.7)$$

$$\Delta\theta_{TO,U} = \Delta\theta_{TO,R} \left(\frac{1 + RK^2}{1 + R} \right)^n \quad (4.8)$$

where

- τ_{TO} is the oil time constant of a transformer.
- $\Delta\theta_{TO,R}$ is the top-oil rise over ambient temperature at rated load. A transformer manufacturer can measure this parameter during a heat run.

- R is the ratio of load loss to no-load loss
- K is the nominal load on the transformer. So, for instance when the apparent power of a $400kVA$ transformer is $200kVA$, $K = 0.5$. The term K_i is the initial condition.
- n is a sort of cooling factor. For ONAN transformers, the guide gives a value of $n = 0.8$.

The IEEE only presents this equation, which is only valid for step-changing load. However, looking more closely at the equation, we see it is a solution to a differential equation. By using the differential equation form of the equation, we can use this equation with varying loads. The differential equation is:

$$\tau_{TO} \frac{d\Delta\theta_{TO}}{dt} = -\Delta\theta_{TO} + \Delta\theta_{TO,U} \quad (4.9)$$

Similarly, for the hot spot to top oil temperature rise $\Delta\theta_H$, they only give the exponential form:

$$\Delta\theta_H = (\Delta\theta_{H,U} - \Delta\theta_{H,i}) \left(1 - \exp \left(-\frac{t}{\tau_w} \right) \right) + \Delta\theta_{H,i} \quad (4.10)$$

with parameters:

$$\Delta\theta_{H,i} = \Delta\theta_{H,R} K_i^{2m} \quad (4.11)$$

$$\Delta\theta_{H,U} = \Delta\theta_{H,R} K^{2m} \quad (4.12)$$

where

- τ_w is the winding time constant of a transformer.
- $\Delta\theta_{H,R}$ is the winding hot spot rise over top-oil temperature at rated load. Transformer manufacturers can measure this parameter during a heat run.
- m is a factor determining the variation of $\Delta\theta_H$ with changing load. For ONAN transformers, the guide gives a value of $m = 0.8$.

The differential equation form of this equation is given by:

$$\tau_w \frac{d\Delta\theta_H}{dt} = -\Delta\theta_H + \Delta\theta_{H,U} \quad (4.13)$$

The transformer manufacturer can measure the top-oil rise over ambient $\Delta\theta_{TO,R}$ and the winding hot spot rise over ambient $\Delta_{H/A,R}$ during a heat run test. The rated value of hot spot rise over top oil is then given by:

$$\Delta\theta_{H,R} = \Delta\theta_{H/A,R} - \Delta\theta_{TO,R} \quad (4.14)$$

4.3. IEC loading guide

The IEC loading guide [34] is a newer and slightly different way to compute the hot spot temperature. The guide presents an exponential method suitable for heat-run tests and a differential method more suitable for variable load and ambient temperature. Consequently, we will only show the differential method here.

Differential equation form

In the IEC equations, the hot spot temperature is a sum of two terms: the top oil temperature and the hot spot temperature rise:

$$\theta_h = \theta_o + \Delta\theta_h \quad (4.15)$$

To determine the top oil temperature, the guide gives almost the same differential equation as derived from the IEEE loading guide:

$$k_{11}\tau_o \frac{d\theta_o(t)}{dt} = \Delta\theta_{or} \left(\frac{1 + R K(t)^2}{1 + R} \right)^x - \theta_0(t) + \theta_a(t) \quad (4.16)$$

where

- $\theta_o(t)$ is the top oil temperature
- $\Delta\theta_{or}$ is the top oil temperature rise at rated load
- $\theta_a(t)$ is the ambient temperature
- R is the ratio of the load to no-load loss
- $K(t)$ is the load factor
- τ_o is the oil time constant
- x is the oil exponent
- k_{11} is a constant

When $k_{11} = 1$, this results in the same equation as Equation 4.9, except that now the ambient temperature is taken inside the differential equation instead of adding it to the solution.

The guide now calculates the hot spot temperature rise by a difference of two differential equations:

$$\Delta\theta_h = \Delta\theta_{h1} - \Delta\theta_{h2} \quad (4.17)$$

In this difference, the first term represents the hot spot temperature rise without considering the effect of the oil flow. The second term is the temperature change because of oil flow, which decreases the temperature.

The differential equations for both terms are given by:

$$k_{22}\tau_w \frac{d\Delta\theta_{h1}(t)}{dt} = k_{21}K(t)^y \Delta\theta_{hr} - \Delta\theta_{h1}(t) \quad (4.18)$$

$$\frac{\tau_o}{k_{22}} \frac{d\Delta\theta_{h2}(t)}{dt} = (k_{21} - 1)K(t)^y \Delta\theta_{hr} - \Delta\theta_{h2}(t) \quad (4.19)$$

where

- k_{21}, k_{22} are constants
- τ_w is the winding time constant
- y is the winding exponent
- $\Delta\theta_{hr}$ is the difference in temperature between the top oil and the hot spot temperature.
As with the IEEE guide, Equation 4.14 calculates this term.

The IEC gives the parameters in Table 4.1 for ONAN distribution transformers.

Name	Variable	Value
Oil exponent	x	0.8
Winding exponent	y	1.6
Constant	k_{11}	1
Constant	k_{21}	1
Constant	k_{22}	2
Time constant	τ_o	180
Time constant	τ_w	4

Table 4.1: Typical values for parameters in distribution transformer (ONAN) [34]

Manufacturers determine the values for R , $\Delta\theta_{or}$ and $\Delta\theta_{hr}$ per transformer during a heat runs test, and these values have to be below specific normative values.

The IEC guide gives only the variables given above for distribution transformers, but these transformers can vary widely in power, size, and cooling capability. Hence, to get a more accurate representation, one can place a top oil thermometer in the transformer, which we can use to determine the variables x , k_{11} and τ_o quantitatively using a parameter estimation algorithm [45].

4.4. Example loading guides

To illustrate what these guides are capable of, we consider one of the transformers actively measured by Stedin. These measurements give the apparent power every 5 minutes, as given in Appendix A. We can obtain the K variable by dividing the apparent power with the rating of 400kVA. Unfortunately, these transformers do not have a top oil thermometer, so the values in Table 4.1 will be used for the IEC loading guide. For the IEEE loading guide, we gave the values in the text. For the remaining parameters, we use a constant ambient temperature of 30°C, $R = 9$, $\Delta\theta_{or} = 55$ and $\Delta\theta_{hr} = 9$. We solve the differential equations using Julia and the numerical `Tsit5()` solver for a small numerical error.

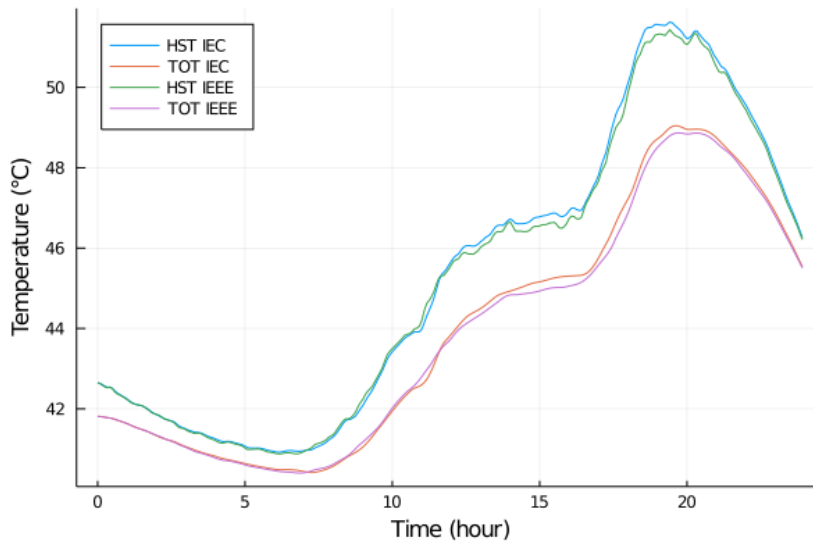


Figure 4.3: Hot spot and top oil temperature for the IEC and IEEE loading guide and the load given in Appendix A.

The slight differences between the two guides are because of how the guides incorporate the ambient temperature in the equations. The IEEE guide adds the ambient temperature to the solution of the differential equation for the top oil temperature. In contrast, the IEC guide incorporates ambient temperature in the differential equation for the top oil temperature. Therefore, the numerical solution to these equations changes slightly.

Assuming a nominal lifespan of $180.000h$, we can calculate the loss of life according to Equation 4.4:

$$LOL = \frac{\sum F_{AA}}{|F_{AA}|} \cdot \frac{24 \cdot 100\%}{180000} = 5.327 \cdot 10^{-6}\% \quad (4.20)$$

Putting this percentage into perspective: if we assume the transformer has this loading pattern from when it was placed until it breaks down, it would last 51393 years.¹

With the program in place, we can do experiments about the influence of certain parameters. For example, varying the exponents x and y in the IEC guide gives the hot spot temperatures in Figure 4.4.

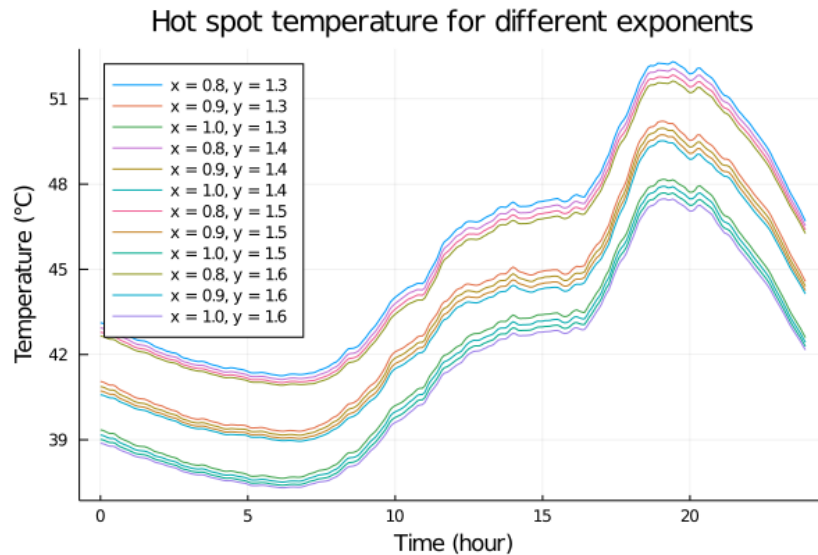


Figure 4.4: Hot spot temperature for different values of the exponents in the IEC loading guide

In this case, the transformer would have a lifetime of 47195 years with the top curve and double that number with the lowest curve. Even though the number of years is enormous, it does tell us something about the sensitivity of the loading guide, as only a tiny change in the exponents gives a massive increase in lifetime.

Extrapolating this to higher loads, we find something strange. Multiplying the K-factor by 3 and rerunning the program gives the hot spot temperatures in Figure 4.5.

¹This calculation comes from: $\frac{\sum F_{AA}}{|F_{AA}|} \frac{x}{180000} = 1 \Rightarrow x \approx 4.505e8 \text{ hours} \approx 51393 \text{ years}$

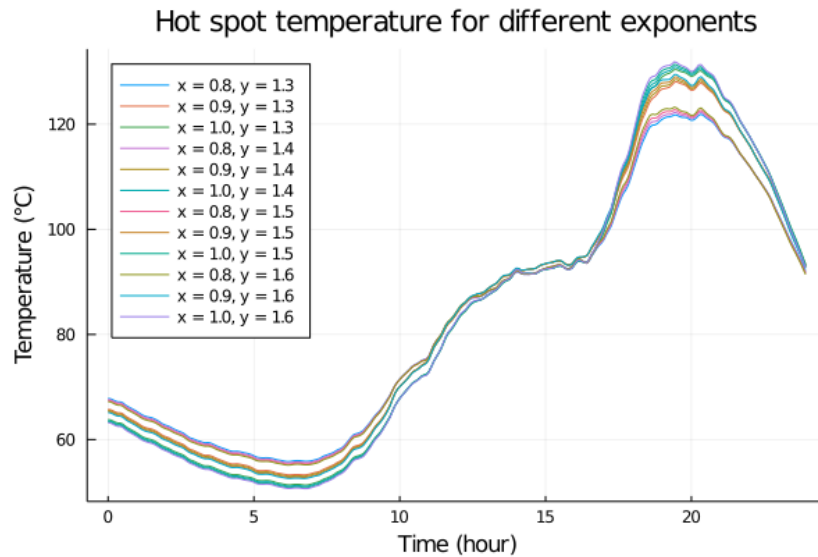


Figure 4.5: Hot spot temperature for different values of the exponents in the IEC loading guide

Here the hot spot temperatures for the exponents switch places. Whereas in Figure 4.4, the curve for $x = 0.8, y = 1.3$ stays on top the whole time, in this case, it switches position at around 90°C , and at $t = 20$, this curve is at the bottom. To explain why this happens, we need to look back at Equation 4.16 and 4.18. When $K < 1$, $\left(\frac{1+RK^2}{1+R}\right)^{0.8} > \left(\frac{1+RK^2}{1+R}\right)^1$ and $K^{1.3} > K^{1.6}$, but when $K > 1$, $\left(\frac{1+RK^2}{1+R}\right)^{0.8} < \left(\frac{1+RK^2}{1+R}\right)^1$ and $K^{1.3} < K^{1.6}$. This relation also tells us the importance of the exponents: when the load is between $K = 0.9$ and $K = 1.1$, the exponents do not really matter as can be seen between $t = 10$ and $t = 17$ in Figure 4.5. However when the load is outside that range the exponents do matter, as the temperature at $t = 20$ ranges between 120°C and 130°C .

What was discussed so far in this chapter only considers the load on the transformer to determine the temperature. However, these guides do not consider the phenomenon of harmonic currents and voltages. Therefore, the IEEE developed another standard to include harmonics in the temperature.

4.5. Including harmonics

The IEEE has developed a different standard to incorporate harmonics into the temperature calculations [46]. This standard introduces loss factors multiplied with estimated eddy current and stray losses. With these newly determined losses, they calculate new values for $\Delta\theta_{or}$ and $\Delta\theta_{hr}$ as mentioned in the previous section.

The standard divides the load losses into two terms:

$$P_{LL-R} = P_{I2R} + P_{TSL-R} \quad (4.21)$$

where

- P_{LL-R} is the rated load loss
- P_{I2R} is the I^2R loss portion of the load loss
- P_{TSL-R} is the rated total stray loss

We can calculate the total rated stray loss with the following equation:

$$P_{TSL-R} = P_{LL-R} - K \cdot (I_1^2 R_1 + I_2^2 R_2) \quad (4.22)$$

where

- P_{TSL-R} is the total stray loss under rated conditions
- P_{LL-R} is the load loss under rated conditions
- K is a constant dependent on the number of phases, $K = 1.5$ for three-phase transformers
- I_1 is the high-voltage RMS (root mean square) fundamental line current under rated frequency and rated load conditions
- R_1 is the resistance measured between two HV terminals
- I_2 is the low voltage RMS fundamental line current under rated frequency and rated load conditions
- R_2 is the resistance measured between two LV terminals

This stray loss consists of the winding eddy current loss and other stray losses. The ratio of the eddy current and other stray losses is experimentally determined per transformer rating. For instance, for a 400kVA transformer winding eddy currents are 50% of the total stray loss and 50% are other stray losses, so:

$$P_{TSL-R} = 0.5P_{EC-R} + 0.5P_{OSL-R} \quad (4.23)$$

The norm then uses the equations above to calculate the rated eddy current and stray losses. When harmonic currents are present, the winding eddy current loss can be calculated by:

$$P_{EC} = P_{EC-R} \frac{\sum_{h=1}^{h_{max}} I_h^2 h^2}{\sum_{h=1}^{h_{max}} I_h^2} \quad (4.24)$$

where

- P_{EC} is the winding eddy-current loss (watts)
- P_{EC-R} is the winding eddy-current loss at the rated current and the power frequency (watts)
- h is the harmonic order
- h_{max} is the highest significant harmonic number
- I_h is the RMS current at harmonic h (amperes)

The harmonic loss factor is then the ratio between the winding eddy current loss and the rated winding eddy current loss:

$$F_{HL} = \frac{P_{EC}}{P_{EC-R}} = \frac{\sum_{h=1}^{h_{max}} I_h^2 h^2}{\sum_{h=1}^{h_{max}} I_h^2} \quad (4.25)$$

Now by dividing each summation by the RMS fundamental load current, only the per-unit value of the harmonics are needed, so:

$$F_{HL} = \frac{\sum_{h=1}^{h_{max}} \left(\frac{I_h}{I_1}\right)^2 h^2}{\sum_{h=1}^{h_{max}} \left(\frac{I_h}{I_1}\right)^2} \quad (4.26)$$

We can obtain a similar factor for the stray losses. However, instead of squaring the harmonic order, it is raised to the power of 0.8. This exponent is conservatively estimated based on experiments. Hence:

$$F_{STR} = \frac{\sum_{h=1}^{h_{max}} \left(\frac{I_h}{I_1} \right)^2 h^{0.8}}{\sum_{h=1}^{h_{max}} \left(\frac{I_h}{I_1} \right)^2} \quad (4.27)$$

With these factors the norm determines new temperature rises. For the top oil temperature rise:

$$\Delta\theta_{or} = \Delta\theta_{or,R} \left(\frac{P_{LL} + P_{NL}}{P_{LL-R} + P_{NL}} \right)^{0.8} \quad (4.28)$$

with

$$P_{LL} = P_{I2R} + F_{HL}P_{EC} + F_{STR}P_{OSL} \quad (4.29)$$

where

- $\Delta\theta_{or}$ is the new top oil temperature rise
- $\Delta\theta_{or,R}$ is the old top oil temperature rise
- P_{LL} is the load losses under the new harmonic load
- P_{NL} is the no-load losses
- P_{LL-R} is the rated no-load losses

For the hot spot rise, only the eddy currents are considered. For a 400kVA transformer, the norm assumes that of the load losses, 40% are in the low voltage winding and that the hottest spot region is four times the average eddy loss [46]. Hence:

$$\Delta\theta_{hr} = \Delta\theta_{hr,R} \left(\frac{1.5 \cdot I_2^2 R_2 + P_{EC} \cdot 0.4 \cdot 4}{P_{I2R} + P_{EC,R}} \right)^{0.8} \quad (4.30)$$

To illustrate the calculation procedure, we use the data from the heat run done for a 400kVA transformer by IEO and the harmonic distribution presented in Figure 2.12. This transformer has the following parameters:

- $R_1 = 1.8131\Omega$ (at 16°C)
- $R_2 = 0.0013\Omega$ (at 16°C)
- $I_1 = 21.48A$
- $I_2 = 549.9A$
- $P_{LL-R} = 3264W$
- $P_{NL-R} = 360W$
- $\Delta\theta_{or,R} = 55^\circ C$
- $\Delta\theta_{hr,R} = 64 - 55 = 9^\circ C$

So the total stray losses are equal to:

$$P_{TSL-R} = 3264 - 1.5 \cdot (21.48^2 \cdot 1.8131 + 549.9^2 \cdot 0.0013) = 3264 - 1844.5 = 1419.5W \quad (4.31)$$

Therefore, according to Equation 4.23, the winding eddy loss and other stray losses are $P_{EC-R} = P_{OSL-R} = 709.8W$.

We can calculate the term in the loss factors for the harmonic distribution of Figure 2.12 in Table 4.2.

h	$\frac{I_h}{I}$	$\left(\frac{I_h}{I}\right)^2$	h^2	$\left(\frac{I_h}{I}\right)^2 h^2$	$h^{0.8}$	$\left(\frac{I_h}{I}\right)^2 h^{0.8}$
1	1	1	1	1	1	1
3	0.4	0.16	9	1.44	2.408	0.385
5	0.2	0.04	25	1	3.623	0.145
7	0.1	0.01	49	0.49	4.743	0.047
Σ		1.21		3.93		1.578

Table 4.2: Harmonic multiplier calculations

We can now obtain the harmonic multipliers using Equation 4.26 and 4.27, so the eddy current multiplier is 3.2479, and the other stray loss multiplier is 1.3038.

Putting all the losses together in a table, and multiplying with the harmonic multiplier, gives Table 4.3.

Type of loss	Rated losses	Harmonic multiplier	Corrected loss
No-load	360		360
P_{I2R}	1844.5		1844.5
P_{EC}	709.8	3.2479	2305.38
P_{OSL}	709.8	1.3038	925.5
Total	3624		5435.28

Table 4.3: Losses before and after the harmonic multiplier

The top oil rise is then equal to:

$$\Delta\theta_{or} = 55 \cdot \left(\frac{5435.28}{3624} \right)^{0.8} = 76.07^\circ C \quad (4.32)$$

And the hot spot rise is equal to:

$$\Delta\theta_{hr} = 9 \cdot \left(\frac{1.5 \cdot 549.9^2 \cdot 0.0013 + 2305.38 \cdot 0.4 \cdot 4}{1844.4 + 709.8} \right)^{0.8} = 13.60^\circ C \quad (4.33)$$

Rerunning the same program like the one in Figure 4.3, but now with the newly determined values for $\Delta\theta_{or}$ and $\Delta\theta_{hr}$ gives the temperatures in Figure 4.6.

As expected, the temperature rises a lot more. In this case, the transformer would last 19622 years, about 2.5 times shorter than in the run without harmonics.

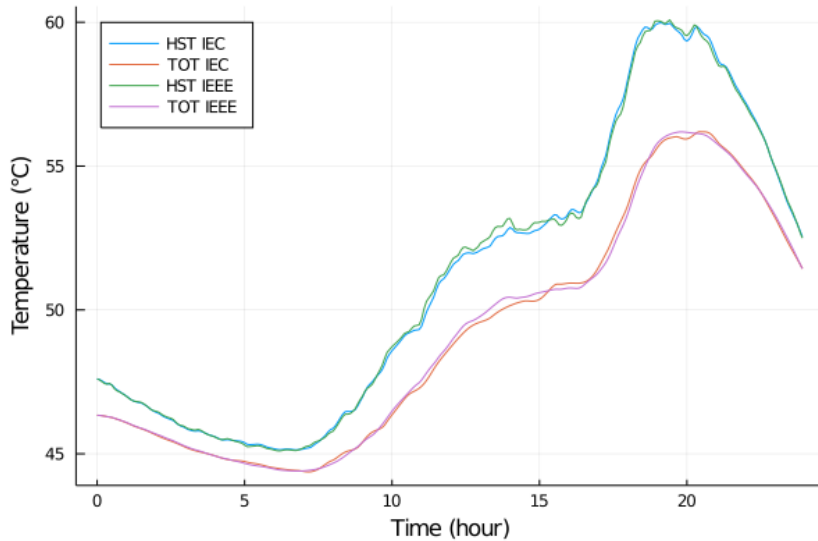


Figure 4.6: Hot spot and top oil temperature with newly determined temperature rise

4.6. Conclusion loading guide

The loading guide can be a valuable tool to give an idea about the temperature and, therefore, the remaining life of a transformer. It provides a way to estimate the hot spot temperature by only needing a few parameters written on the transformer's nameplate. It can also serve as the first step towards a digital twin of a transformer, as it gives a real-time evaluation of one of the most critical variables in a transformer: the temperature. Additionally, we can make predictions with the loading guide: say we have a particular loading pattern for the next ten years, then what would be the reduction of life in that time?

However, the loading guide also has some downsides, primarily based on this model's generality. Although distribution transformers can vary widely in rating, size and location, both the IEEE and IEC guide only give one set of values for the parameters. As a result, these parameters can cause an over-or underestimation of the actual temperature in the transformer, which in both cases can lead to more costs.

Additionally, the loading guide does not say anything about when this transformer will reach the end of its life since the transformer was not measured and monitored since Stedin placed it. To account for this problem, one could use average household usage for every year the transformer was in operation, add all the houses in a neighbourhood together to get the load over the transformer, and apply the loading guide to this loading data. This method can give a rough idea of how much life the transformer has previously lost and therefore provide an initial condition for the remaining life of the transformer when it is measured.

Lastly, when including harmonics into the guide, many assumptions are made about the distribution of the losses, the exponents, and how these losses affect the temperature rises. Furthermore, when including harmonics, the windings' resistance is also needed. Manufacturers determine the resistance during a heat run test, but this number is often not written onto the transformer's nameplate and is therefore unavailable to Stedin.

The next chapter introduces the Maxwell equations with which we can model the losses due to harmonics analytically to circumvent some of these problems. Additionally, we explain how these losses can be coupled to a heating term in a multiphysics approach.

5

Theoretical background first principles model

In the previous chapter, we saw that the loading guide determines the hot spot temperature and, in turn, the remaining life under a specific load profile. However, in the end, we made multiple remarks about the validity of the Loading Guide for our area of study. For example, we are studying distribution transformers, which can vary widely in rating and size, but the loading guide only gives one set of parameters for all distribution transformers.

Another point is that the loading guide is empirical. For example, one of the assumptions is that the oil temperature rises linearly from the bottom to the top of the oil tank, but realistically this is not the case as there are all kinds of non-linearities in the oil flow. Additionally, the guide assumes that the hot spot temperature is at some fixed multiple of the temperature at the top of the winding. However, this temperature can vary widely depending on the build of the transformer and load on it.

The idea is now to model the transformer more analytically and model the behaviour described in Chapter 3 to combat some of these problems. In this way, we can better consider the different effects of harmonics and temperature rises. However, for the sake of time in this research, only the electromagnetic effects are modelled using Maxwell's equations. Also, the model will be a 2D model of the cross-section of a transformer. Therefore, we will simplify the potential formulations to a single 2D partial differential equation.

The electromagnetic effects can be described analytically by Maxwell's equations. People have written multiple books about the intricacies of Maxwell's equations, so in this chapter, we will discuss only the most important results [12]. This chapter describes the theoretical background needed for the model developed in the next chapter. It starts with the different forms of Maxwell's equations. These forms need initial, and boundary conditions and the resulting equations are solved using the finite element method. Next, the different ways of the coil excitation are discussed, which can be current or voltage driven. Then we discuss the constitutive parameters and how we model them. Lastly, this chapter describes the different ways of determining the losses and shows how we can incorporate these losses into the heat equation.

5.1. Study types

This section presents the various equations, which are the basis for the finite element method for different study types.

Time-dependent

The most general form of the Maxwell equations, where all bold symbols are functions in time and space e.g. $\mathbf{E} = \mathbf{E}(\mathbf{x}, t)$, is given by:

$$\nabla \times \mathbf{E} = -\frac{\partial \mathbf{B}}{\partial t} \quad (5.1)$$

$$\nabla \times \mathbf{H} = \mathbf{J} + \frac{\partial \mathbf{D}}{\partial t} \quad (5.2)$$

$$\nabla \cdot \mathbf{B} = 0 \quad (5.3)$$

$$\nabla \cdot \mathbf{D} = \rho \quad (5.4)$$

where:

- \mathbf{E} , [V/m] is the electric field intensity.
- \mathbf{H} , [A/m] is the magnetic field intensity.
- \mathbf{J} , [A/m^2] is the current density.
- \mathbf{B} , [T] is the magnetic flux density.
- \mathbf{D} , [C/m^2] is the electric flux density.
- ρ , [C/m^3] is the free charge density.

with corresponding constitutive relations:

$$\mathbf{J} = \mathbf{J}_e + \mathbf{J}_{cond} \quad (5.5)$$

$$\mathbf{B} = \mu \mathbf{H} \quad (5.6)$$

$$\mathbf{J}_{cond} = \sigma \mathbf{E} \quad (5.7)$$

$$\mathbf{D} = \epsilon \mathbf{E} \quad (5.8)$$

where

- \mathbf{J}_e is the external current density, the amount of current passing through a surface.
- \mathbf{J}_{cond} is the conductive current density, the amount of current on a surface.
- σ , [S/m] is the electrical conductivity, a measure of the ability of a material to conduct electric current.
- $\mu = \mu_0 \mu_r$, [H/m] is the permeability, with $\mu_0 = 4\pi \cdot 10^{-7}$ the permeability of free space and μ_r the relative permeability of the material, a measure of the ability of a material to magnetize in response to a magnetic field.
- $\epsilon = \epsilon_0 \epsilon_r$, [F/m] is the permittivity, with $\epsilon_0 = \mu_0^{-1} c^{-2}$ the vacuum permittivity and ϵ_r the relative permittivity of the material, a measure of the ability of a material to electrically polarize. Since the term ϵ_0 is very small ($\mathcal{O}(10^{-12})$) and for all materials considered in this research $\epsilon_r < 10$, this term is neglected in the rest of this research.

All three parameters have more to them than being just a number, and we will further discuss the permeability and conductivity in Section 5.3. Filling in the constitutive relations and rearranging yields:

$$\nabla \times \mathbf{E} = -\frac{\partial \mathbf{B}}{\partial t} \quad (5.9)$$

$$\nabla \times \mu^{-1} \mathbf{B} = \mathbf{J}_e + \sigma \mathbf{E} \quad (5.10)$$

$$\nabla \cdot \mathbf{B} = 0 \quad (5.11)$$

To solve this set of equations, we use the potential formulation. We can derive this formulation from the fact that the divergence of the curl of a vector field is zero. Therefore, Equation 5.11 is written as:

$$\mathbf{B} = \nabla \times \mathbf{A} \quad (5.12)$$

Filling this in, in Equation 5.9, we obtain:

$$\nabla \times \mathbf{E} = -\frac{\partial(\nabla \times \mathbf{A})}{\partial t} \quad (5.13)$$

This equation is valid if we define:

$$\mathbf{E} = -\nabla \varphi - \frac{\partial \mathbf{A}}{\partial t} \quad (5.14)$$

for any continuous, twice differentiable scalar φ since

$$\nabla \times \mathbf{E} = \nabla \times \left(-\nabla \varphi - \frac{\partial \mathbf{A}}{\partial t} \right) = -\nabla \times (\nabla \varphi) - \frac{\partial(\nabla \times \mathbf{A})}{\partial t} = -\frac{\partial(\nabla \times \mathbf{A})}{\partial t} \quad (5.15)$$

Now combining Equation 5.10, 5.12, 5.14 yields:

$$\nabla \times (\mu^{-1} \nabla \times \mathbf{A}) = \mathbf{J}_e + \sigma \left(-\nabla \varphi - \frac{\partial \mathbf{A}}{\partial t} \right) \quad (5.16)$$

$$= \mathbf{J}_e - \sigma \nabla \varphi - \sigma \frac{\partial \mathbf{A}}{\partial t} \quad (5.17)$$

Since we ignore Equation 5.4, there is only one equation, but we have two unknowns: φ and \mathbf{A} . However, we can choose any twice differentiable scalar field for φ , so for simplicity, we set $\varphi = 0$. In the 2D case we can let $\mathbf{A} = (0, 0, A_z(t, x, y))$ and $\mathbf{J}_e = (0, 0, J_z(t, x, y))$ and this equation simplifies to:

$$-\frac{\partial}{\partial x} \left(\mu^{-1} \frac{\partial A_z}{\partial x} \right) - \frac{\partial}{\partial y} \left(\mu^{-1} \frac{\partial A_z}{\partial y} \right) + \sigma \frac{\partial A_z}{\partial t} = J_z \quad (5.18)$$

At this point, we have the time-dependent potential formulation that we can use for our finite element calculation.

Frequency domain

With an alternating current, we are dealing with a current that changes 50 times a second. So, we would have to take steps of 0.001 seconds or smaller to represent the electromagnetic behaviour accurately. However, the temperature in the transformer changes on a scale of minutes, meaning that we would need $1000 \cdot 60 \cdot 10 = 600.000$ time steps to calculate the change in temperature over 10 minutes. Yet, for most of the calculations, nothing happens to the temperature at all. To solve this problem, we can reformulate the Maxwell equations by

assuming that every variable behaves periodically with the same frequency. Therefore, we can put Maxwell's equations into phasor form [47]. If we then set:¹

$$\mathbf{E}(\mathbf{x}, t) = \operatorname{Re}\{e^{i\omega t} \mathcal{E}(\mathbf{x})\} \quad (5.19)$$

$$\mathbf{B}(\mathbf{x}, t) = \operatorname{Re}\{e^{i\omega t} \mathcal{B}(\mathbf{x})\} \quad (5.20)$$

$$\mathbf{J}_e(\mathbf{x}, t) = \operatorname{Re}\{e^{i\omega t} \mathcal{J}(\mathbf{x})\} \quad (5.21)$$

and fill this in in Equation 5.9, 5.10 and 5.11, we get:

$$\nabla \times \mathcal{E} = -i\omega \mathcal{B} \quad (5.22)$$

$$\nabla \times \mu^{-1} \mathcal{B} = \mathcal{J} + \sigma \mathcal{E} \quad (5.23)$$

$$\nabla \cdot \mathcal{B} = 0 \quad (5.24)$$

Applying the same trick to the vector potential, so $\mathbf{A}(\mathbf{x}, t) = \operatorname{Re}\{e^{i\omega t} \mathcal{A}(\mathbf{x})\}$, gives for Equation 5.12 and 5.14:

$$\mathcal{B} = \nabla \times \mathcal{A} \quad (5.25)$$

$$\mathcal{E} = -\nabla \varphi - i\omega \mathcal{A} \quad (5.26)$$

Filling in these equations in the equations above gives:

$$\nabla \times (\mu^{-1} \nabla \times \mathcal{A}) = \mathcal{J} + \sigma(-\nabla \varphi - i\omega \mathcal{A}) \quad (5.27)$$

$$= \mathcal{J} - \sigma \nabla \varphi - \sigma i\omega \mathcal{A} \quad (5.28)$$

This can again be simplified if we choose the scalar potential to be zero, so $\varphi = 0$, and if we let $\mathcal{A} = (0, 0, A_z(x, y))$ and $\mathcal{J} = (0, 0, J_z(x, y))$ this reduces down to:

$$-\frac{\partial}{\partial x} \left(\mu^{-1} \frac{\partial A_z}{\partial x} \right) - \frac{\partial}{\partial y} \left(\mu^{-1} \frac{\partial A_z}{\partial y} \right) + \sigma i\omega A_z = J_z \quad (5.29)$$

Initial and boundary condition

To solve Equation 5.18 and 5.29, we need one more thing: a boundary condition. We will assume in our model that no magnetic flux will pass through the boundary, also called magnetic insulation, which is mathematically given by:

$$\mathbf{B} \cdot \mathbf{n} = 0 \quad (5.30)$$

In potential formulation, this is equal to:

$$0 = (\nabla \times \mathbf{A}) \cdot \mathbf{n} = \nabla \cdot (\mathbf{n} \times \mathbf{A}) \Rightarrow \mathbf{n} \times \mathbf{A} = 0 \quad (5.31)$$

For Equation 5.18 we need, an initial condition and a boundary condition. To make things easy, we set:

$$\mathbf{A}(0, \mathbf{x}) = 0 \quad (5.32)$$

¹In some cases, the complex symbol is given by j , as the symbol for the current is also i , but since the writer is a mathematician, we use i as the complex symbol

Finite Element Method

We want to solve 5.18 and 5.29 with the abovementioned boundary and initial conditions over an inhomogeneous domain with different values for μ , σ , and J_z for different parts of the domain. To accomplish this, we use the finite element method [48]. The finite element method is a numerical approximation method that discretizes the domain on which it solves the (partial) differential equations into triangular or quadrilateral elements. The method then solves the equations for each of these elements and combines the results.

We use a finite element method to solve these equations as this method can handle complex domains without us modifying the formulation or computer code [49]. Also, the matrices created from a finite element method are highly sparse or have a banded structure, making the final equation computationally easier to solve.

5.2. Coil excitation

One term is present in all equations above and acts as a source term: \mathbf{J}_e . This term is the external current density, which in our case is only present in the transformer's coils. To model these coils, we use the option of a homogenized multi-turn coil in COMSOL. With this option, we can set a rectangle (in 2D) or a cylinder (in 3D) as the coil without individually modelling each wire, saving computation time. Furthermore, the coil can be excited in two ways: current driven and voltage-driven.

Current driven

Mathematically a current-driven coil is given by

$$\mathbf{J}_e = \frac{NI_{coil}}{A} \mathbf{e}_{coil} \quad (5.33)$$

where:

- \mathbf{J}_e is the external current density
- N is the number of turns in the winding
- I_{coil} is the given coil current
- A is the area of the winding, defined by the geometry
- \mathbf{e}_{coil} is the unit vector of the excitation direction

With a current-driven coil, we only have to set the coil current I_{coil} and then the finite element solver will solve the potential over our domain. However, things get a bit trickier for a voltage-driven coil, which we will discuss next.

Voltage driven

For a voltage-driven coil we start with the same equation as with a current-driven coil, so:

$$\mathbf{J}_e = \frac{NI_{coil}}{A} \mathbf{e}_{coil} \quad (5.34)$$

However, now we want to determine I_{coil} in a different way. We want the voltage to be a sum of the resistive current and the induced current. The resistive current is given by Ohms law: $V = IR$. So, in this case, the total voltage is equal to:

$$V_{tot} = I_{coil}R_{coil} + V_{ind} \quad (5.35)$$

With

$$V_{ind} = \frac{1}{A} \iint_A (\mathbf{E} \cdot \mathbf{e}_{coil}) \cdot N \cdot L \, dA \quad (5.36)$$

$$R_{coil} = \frac{1}{A} \iint_A \frac{N \cdot L}{\sigma_{coil} a_{coil}} \, dA \quad (5.37)$$

where

- \mathbf{J}_e is the external current density
- N is the number of turns in the winding
- V_{tot} is the total voltage. This variable is imposed
- V_{ind} is the induced voltage
- A is the area of the winding, defined by the geometry
- R_{coil} is the total resistance of the coil
- \mathbf{e}_{coil} is the unit vector of the excitation direction
- \mathbf{E} is the electric field
- L is in 2D the out of plane thickness, and in 3D, the thickness of the coil winding
- σ_{coil} is the coil wire conductivity
- a_{coil} is the coil wire cross-section area

In 2D V_{ind} can be simplified to:

$$V_{ind} = \frac{1}{A} \iint_A E_z \cdot N \cdot L \, dA \quad (5.38)$$

where $E_z = -\frac{\partial A_z}{\partial t}$ in the time domain and $E_z = -i\omega A_z$ in the frequency domain.

Now substituting Equation 5.34 and 5.35 into Equation 5.29, gives:

$$-\frac{\partial}{\partial x} \left(\mu^{-1} \frac{\partial A_z}{\partial x} \right) - \frac{\partial}{\partial y} \left(\mu^{-1} \frac{\partial A_z}{\partial y} \right) + \sigma i\omega A_z = \frac{N(V_{tot} - V_{ind})}{A \cdot R} \quad (5.39)$$

However, when filling in the equation for V_{ind} , the variable A_z is present on both sides of the equation, with no simple way to bring it to one side. Therefore, we introduce a new equation to be able to solve this:

$$-\frac{\partial}{\partial x} \left(\mu^{-1} \frac{\partial A_z}{\partial x} \right) - \frac{\partial}{\partial y} \left(\mu^{-1} \frac{\partial A_z}{\partial y} \right) + \sigma i\omega A_z = \frac{NI_{coil}}{A} \quad (5.40)$$

$$I_{coil} = \frac{V_{tot} - V_{ind}}{R} \quad (5.41)$$

In this way, we introduce a new equation for each voltage-driven coil in the function resulting from the finite element algorithm.

5.3. Constitutive parameters

We have discussed all the equations needed to solve the electromagnetic field. The only thing still needed now is to model the constitutive parameters given in Equation 5.6 and 5.7.

5.3.1. B-H relation

In its most basic form, we can write the B-H relation as:

$$\mathbf{B} = \mu \mathbf{H} \quad (5.42)$$

Relative permeability

Modelling the permeability with a relative permeability is the simplest case of permeability. In this case, we have that $\mu = \mu_0 \mu_r$, where μ_0 is the vacuum permeability with $\mu_0 = 4\pi \cdot 10^{-7} H/m$ and μ_r the relative permeability, which is different for all materials. For instance, for iron, this value equals 4000, whereas, for air and copper, its value is equal to 1.

$$\mathbf{B} = \mu_0 \mu_r \mathbf{H} \quad (5.43)$$

Modelling the permeability like this linear relationship neglects the electromagnetic effects in ferromagnetic materials such as saturation and hysteresis.

Magnetic losses

To consider the effect of hysteresis loss, one could model the permeability by a complex relative permeability. As discussed in Section 3.1, when applying an alternating magnetic field \mathbf{H} to a material, the associated flux density \mathbf{B} can not keep up with the alternations and lags behind. In mathematical terms, we can write both the magnetic field \mathbf{H} and the flux density \mathbf{B} into complex functions [31]. So:

$$H = H_0 e^{i\omega t} \quad B = B_0 e^{i(\omega t - \delta)} \quad (5.44)$$

Where δ is the phase angle, so how far the flux is behind the field intensity due to hysteresis. We can then determine the complex permeability by dividing B by H :

$$\mu = \frac{B}{H} = \frac{B_0 e^{i\omega t - i\delta}}{H_0 e^{i\omega t}} = \frac{B_0}{H_0} e^{-i\delta} = \frac{B_0}{H_0} \cos \delta - i \frac{B_0}{H_0} \sin \delta = \mu' - i\mu'' \quad (5.45)$$

The real part of this term represents the part of \mathbf{B} that is in phase with \mathbf{H} , and the complex term, μ'' , represents the part of \mathbf{B} that is 90° out of phase with \mathbf{H} .

B-H curve

To incorporate the saturation effects into the core losses, one can model the B-H relation with a B-H curve. In this case, the permeability is given by a non-linear function, mathematically represented by:

$$\mathbf{B} = f(\|\mathbf{H}\|) \frac{\mathbf{H}}{\|\mathbf{H}\|} \quad (5.46)$$

The function f is different for different types of material, as illustrated in Figure 5.1. However, even the same kind of material has different B-H curves. Therefore, the manufacturers do measurements on their materials to obtain this specific curve.

A B-H curve neglects the effects of hysteresis in the B-H relation. However, in this case, one can use the a posteriori Steinmetz equation to determine these losses. We will explain the Steinmetz equation later in Section 5.4. To a priori model both the hysteresis and saturation effects, one can use the Jiles-Atherton model in a time-domain study, but we will not consider that approach in this study.

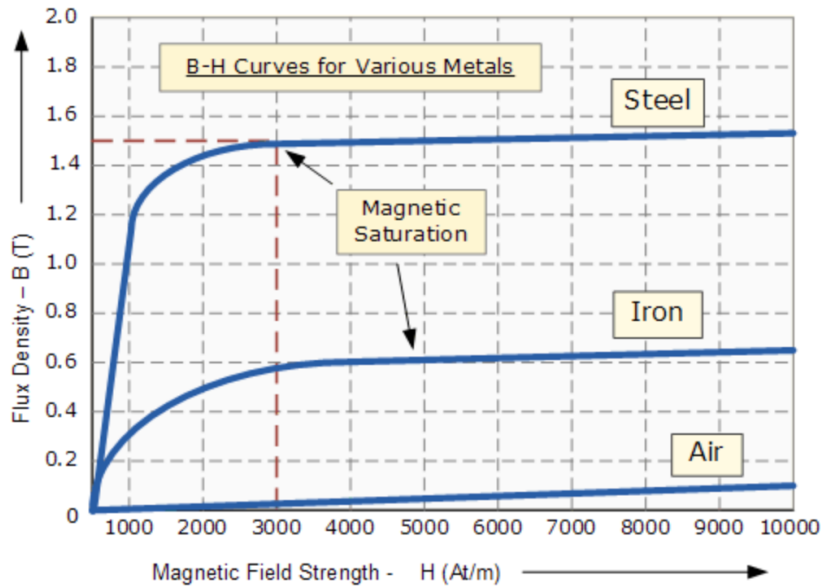


Figure 5.1: Different B-H curves for different types of materials [50]

Effective B-H curve

When modelling in the frequency domain, we must consider that we are not modelling the alternations in the current individually. Therefore the B-H curve also changes. Luckily, COM-SOL made an application to take the cycle average of a given B-H curve to obtain the effective B-H curve [51]. Mathematically, this relation is then given by:

$$\mathbf{B} = f_{eff}(\|\mathbf{H}\|) \frac{\mathbf{H}}{\|\mathbf{H}\|} \quad (5.47)$$

5.3.2. Conductivity

The conductivity of a material is a measure of how easy a current can flow through a material. For instance, electrical steel used in the transformer core has a conductivity of $2.17 \cdot 10^6 \text{ S/m}$, whereas air has a conductivity of $10 \cdot 10^{-10} \text{ S/m}$. There are two ways to model the conductivity: isotropic and anisotropic.

Isotropic conductivity

In the isotropic case, the conductivity is a real number. So, for instance, the conductivity for electric steel would be equal to $2.17e6 \text{ S/m}$. However, this is the value for a single sheet of steel, but in a transformer, the core consists of very thin steel sheets, as visualized in Figure 3.2, to minimize the eddy currents. However, the sheets are so thin that it is impossible to model them individually. Therefore they are often modelled in groups, or the core is modelled as one single block of steel. As a result, both the groups of steel sheets and the single block will have a significantly lower value for the conductivity of the core.

Anisotropic conductivity

Another option to model the conductivity of the core is by making the conductivity anisotropic. In this way, we can set a different value for the conductivity in each direction. However, since the model will be 2D, and the laminations are in the dimension not considered, we cannot apply this option here.

5.4. Losses

We can calculate the losses mentioned in the previous sections from the electromagnetic effects described in Section 3.1.

Core loss

We can calculate the core loss in two ways. The most common way is by using the a posteriori Steinmetz equation. Another option is using the terms introduced by COMSOL for a multiphysics coupling. However, we must note that in both cases, it is challenging to calculate the losses because the losses cause heat in the transformer, which influences the permeability and conductivity of the material, which affects the losses, and so on. Also, as we are modelling transformers that are already in service, not much information is still available about the type of steel used in these transformers.

Steinmetz

The Steinmetz equation was experimentally derived in 1890 [52]. This equation estimates the energy loss due to hysteresis effects and is given by:

$$P_h = k_h f B_m^\beta \quad (5.48)$$

Where P_h is the loss due to hysteresis, f is the frequency, B_m is the magnetic flux density and k_h , and β are parameters that we can determine with curve fitting. However, it is difficult to distinguish whether losses originate from the effects of hysteresis or eddy currents in practice [29]. Therefore, a more general Steinmetz equation is used:

$$P_{fe} = K_c f^\alpha B^\beta \quad (5.49)$$

The core material manufacturers then measure the flux losses for different flux densities for a set frequency (50 or 60Hz), and from this curve, we can determine the parameters K_c , α and β . This equation results in the per volume iron loss, so we need to take the volume integral of this number to calculate the loss over the whole core. For our 2D model, this will mean taking a surface integral and multiplying with the out of plane thickness L .

Unfortunately, this equation only works when we are dealing with sinusoidal waveforms. However, when considering harmonics, the current is a sum of sinusoidal functions, which is a non-sinusoidal function. Therefore, people have developed the improved generalized Steinmetz equation (iGSE) to deal with non-sinusoidal waveforms, as given by the following equation:

$$P = \frac{1}{T} \int_0^T k_i \left| \frac{dB}{dt} \right|^\alpha (\Delta B^{\beta-\alpha}) dt \quad (5.50)$$

where ΔB is the flux density from peak to peak, and k_i is defined by

$$k_i = \frac{K_c}{(2\pi)^{\alpha-1} \int_0^{2\pi} |\cos\theta|^\alpha 2^{\beta-\alpha} d\theta} \quad (5.51)$$

However, since we have to take the time derivative of the magnetic flux density, this equation is only valid in the time domain. Therefore, we will not consider this equation when calculating the losses in the transformer core.

Multiphysics coupling COMSOL

Another option to model the core losses is using the equations that COMSOL uses in their multiphysics coupling with temperature. They divide the core losses into two: resistive losses and magnetic losses. The resistive losses are given by [53]:

$$Q_{rh} = \frac{1}{2} \operatorname{Re}(\mathcal{J} \cdot \bar{\mathcal{E}}) \quad (5.52)$$

Where $\bar{\mathcal{E}}$ is the complex conjugate of \mathcal{E} .

For the magnetic losses, we write \mathcal{B} and \mathcal{H} as in Equation 5.44, so:

$$\mathcal{H} = H_0 e^{i\omega t} \quad \mathcal{B} = B_0 e^{i(\omega t - \delta)} \quad (5.53)$$

The magnetic losses are then given by:

$$Q_{ml} = \frac{1}{2} \operatorname{Re}(\mathcal{B} \cdot \bar{\mathcal{H}} i\omega) \quad (5.54)$$

When \mathcal{B} and \mathcal{H} are in phase with one another, so when $\delta = 0$, this equation is equal to zero. However, if we model the permeability using a complex permeability, as in Equation 5.45, we implicitly set $\delta \neq 0$. Therefore, we can use this equation to calculate the losses in this case.

Integrating Equation 5.52 and 5.54 over the surface of the domain times the out of plane thickness (2D) or integrating over the volume of the domain (3D), gives the power loss in watt.

Winding losses

In comparison with the core losses, the losses in the windings are relatively simple to calculate as there is only one equation to do so:

$$P = I^2 \cdot R \quad (5.55)$$

Where R is the resistance of the coil as given by Equation 5.37. However, this equation changes slightly because we are dealing with complex currents and voltages. In this case, we have resistive losses in the winding. So

$$Q_{rh} = \frac{1}{2} \operatorname{Re}(\mathcal{J} \cdot \bar{\mathcal{E}}) = \frac{1}{2\sigma} \mathcal{J} \cdot \bar{\mathcal{J}} \quad (5.56)$$

However, this equation is valid if we have a homogenized domain as the coils. Unfortunately, this is not the case, as the coils consist of the windings and the paper insulation material. Therefore, we integrate Equation 5.56 over the volume and are left with:

$$P = \frac{1}{2} I_{coil} \cdot \overline{I_{coil}} \cdot R \quad (5.57)$$

The reader can find an explanation of why there is a factor $\frac{1}{2}$ in front of the three terms above in Appendix B.

5.5. Heating

To determine the temperature distribution in the transformer, we can introduce the heat equation in the model, given by:

$$\rho C_p \frac{\partial T}{\partial t} + \rho C_p u \cdot \nabla T = \nabla \cdot (k \nabla T) + Q \quad (5.58)$$

where

- C_p is the heat capacity of a material
- $T(t, \mathbf{x})$ is the temperature at a certain place \mathbf{x} at time t
- ρ is the density of the material
- u is the velocity of the material
- k is the thermal conductivity of a material
- Q is a heat source per unit volume

The only material that moves in a transformer is oil. However, the cooling process mainly happens because of conduction in distribution transformers, as the oil moves little to none. Therefore, if we assume that $u = 0$, we can simplify the equation to:

$$\rho C_p \frac{\partial T}{\partial t} = \nabla \cdot (k \nabla T) + Q \quad (5.59)$$

The heat source is the power per unit volume, which is the same unit as in the Steinmetz equation, but for the winding losses, we need to divide the losses by the volume to get the heat source.

We have now discussed all equations and tools needed to set up a basic transformer model. In the next chapter, we will develop this model.

6

Model runs

Now that we discussed all the theoretical background in the previous chapter, in this chapter, we set up the geometry, determine the mesh and give the other parameters needed for the model. Then, with all the tools at hand, we will explain the build-up of the model and calculate the core and winding losses. Lastly, these losses are also calculated for higher frequencies to determine the effect of harmonics on the losses. The model is developed using COMSOL Multiphysics ®.

6.1. Geometry

We base the geometry on drawings supplied by transformer manufacturer IEO. Unfortunately, these drawings did not mention all dimensions. For example, they did not give the thickness of the windings, so these and other parameters have to be estimated. The model will be 2D, so the geometry will be the same as when we cut a transformer in half along the long direction. Figure 6.1 shows this geometry, where the orange parts are the high voltage windings, the yellow parts the low voltage windings and the purple part the steel core. We have to imagine that the windings on either side of the core leg are connected as, in reality, they form a continuous loop around a leg of the transformer. We slightly rounded the inner corners in Figure 6.1 to prevent numerical singularities from occurring.

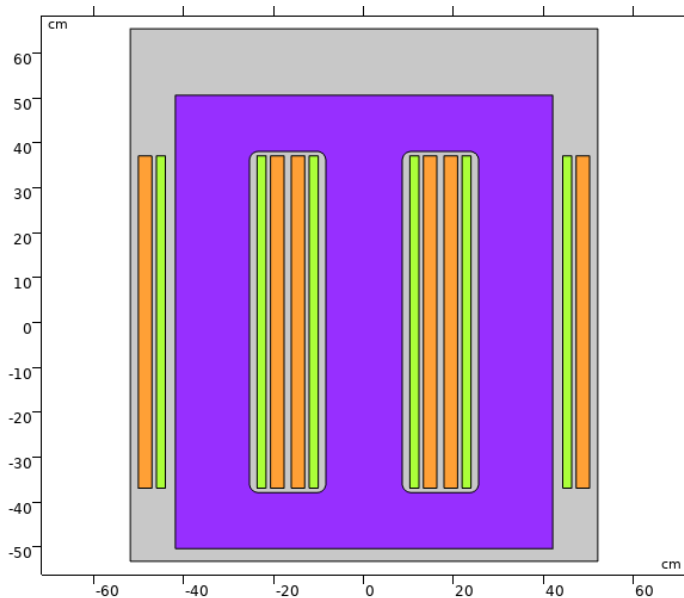


Figure 6.1: 2D geometry of the transformer. The orange and yellow rectangles are the high and low voltage windings, respectively, the purple part is the steel core, and the grey parts are the transformer oil. The white part is the air around the transformer, which we do not consider in this study.

6.2. Mesh

We will use the finite element method to solve the equations mentioned in the previous chapter. Besides the equations and the domain on which we will solve these equations, we need one other thing: a mesh. This mesh divides the domain into tiny elements, and the finite element method solves the equation for every element. As a starting point for finite element simulations, the mesh is divided into triangular-shaped elements, as given in Figure 6.2.

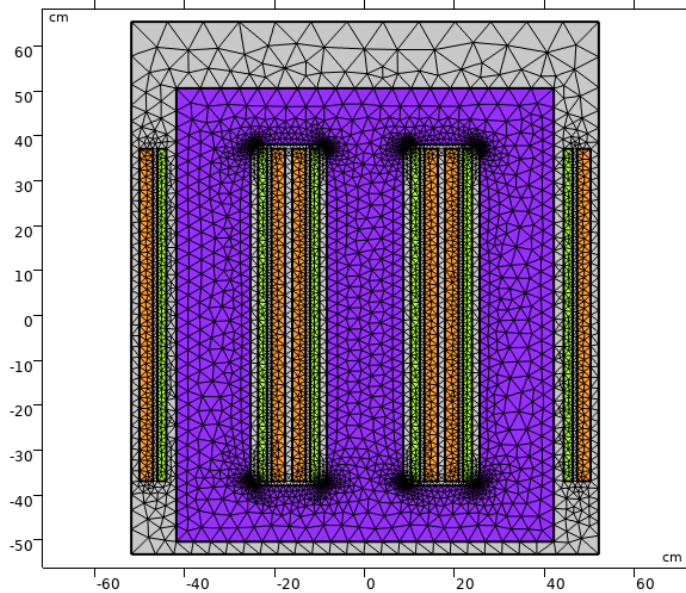


Figure 6.2: Unstructured triangular mesh generated using default settings

6.3. Coil excitation and material coefficients

We can now solve Equation 5.18 and 5.29 using the finite element method with the geometry and mesh setup. However, as mentioned in the previous chapter, these equations need some parameters.

First and foremost, parameters are needed to excite the coils. As discussed, we can do this in two ways: current driven and voltage-driven. In both the time and frequency domain studies, the amplitude of the current and voltage is needed instead of the usually considered RMS values. The considered transformer is a 400kVA transformer with 10750V on the primary and 420V on the secondary side. We can use the following equation to convert between voltages and currents:

$$I = \frac{S}{\sqrt{3}V} \quad (6.1)$$

Where I is the RMS line current, S is the apparent power, and V is the RMS line voltage. Thus, the primary and secondary line currents are:

$$I_{prm,line,rms} = 21.48A \quad (6.2)$$

$$I_{sec,line,rms} = 549.86A \quad (6.3)$$

To convert the line current and voltage to phase current and voltage, we need to take into

account that we are dealing with a delta-wye connected transformer. So by [54]:

$$V_{prm,phase,rms} = 10750V \quad (6.4)$$

$$V_{sec,phase,rms} = \frac{420}{\sqrt{3}} = 242.49V \quad (6.5)$$

$$I_{prm,phase,rms} = \frac{21.48}{\sqrt{3}} = 12.40A \quad (6.6)$$

$$I_{sec,phase,rms} = 549.86A \quad (6.7)$$

These values are still in RMS terms. However, for frequency and time domain calculations, we need the peak values. Hence, by Equation 2.6, all these values need to be multiplied by $\sqrt{2}$ to get the peak amplitudes:

$$V_{prm,phase,peak} = 10750V \cdot \sqrt{2} = 15202.40V \quad (6.8)$$

$$V_{sec,phase,peak} = 242.49V \cdot \sqrt{2} = 342.93V \quad (6.9)$$

$$I_{prm,phase,peak} = 12.40A \cdot \sqrt{2} = 17.54A \quad (6.10)$$

$$I_{sec,phase,peak} = 549.86A \cdot \sqrt{2} = 777.62A \quad (6.11)$$

These will be values for I_{coil} as given in Equation 5.33 or V_{tot} as given in Equation 5.35. In these equations we also need the number of windings in each winding. These can be obtained by first determining the winding ratio using Equation 2.24. So:

$$\frac{V_{prm,phase}}{V_{sec,phase}} = \frac{15202.40}{342.93} = 44.33 = \frac{777.62}{17.54} = \frac{I_{sec,phase}}{I_{prm,phase}} \quad (6.12)$$

Hence, for every secondary winding, 44.33 primary windings are needed. However, that equation is only valid when the power at the primary side is equal to the power at the secondary side. This is not the case since losses occur in the transformer. Unfortunately, the documentation from IEO does not give the exact number of windings on each side, so we will have to use this ratio. Hence, we will use $N_p = 266$ and $N_s = 6$.

If we use the COMSOL calculations for the voltage-driven coils as given in Equation 5.35 to 5.37, we need three other variables for the coils: their cross-section area, their wire conductivity, and their length. However, the IEO documentation did not contain these parameters, so we would have to make a lot of estimations about these parameters. Luckily, the documentation did provide the resistance of the wires based on measurements. Therefore, we can ignore Equation 5.37 and fill in the measured value. However, this is the resistance of a single wire, and we are modelling the combination of wires and paper insulation material. This means that the total resistance of the rectangle we are modelling will be higher since the paper has a higher resistance than aluminium. Therefore, we will introduce a “coil fill factor”, CFF , indicating how much of the rectangle defined in the geometry consists of the windings and how much is paper insulation. So Equation 5.41 gets modified into:

$$I_{coil} = \frac{(V_{tot} - V_{ind}) \cdot CFF}{R} \quad (6.13)$$

With $R = 1.8131 \Omega$ and $CFF = 0.3$ for the primary coils and $R = 1.2999 m\Omega$ and $CFF = 0.3$ for the secondary coils.

We still need one more variable for the voltage-driven coils: the out of plane thickness L . Therefore, it needs to be taken into account that, in reality, the coils are around the core legs.

Also, the secondary windings are enclosed by the primary windings, so the circumference of the secondary windings will be smaller than the primary windings. However, we cannot consider these aspects in the 2D equations underlying COMSOL, as we can only give one value for L . Therefore, based on the drawing supplied by IEO, $L = 40\text{cm}$ is chosen.

The last parameters needed are the material parameters. In our case, we have divided the domain into three materials: the steel core, the aluminium windings and the transformer oil. All of which have different values for the permeability and the conductivity, as given in Table 6.1. In reality, both the permeability and the conductivity are functions of temperature, but we will not consider that in this research. Also, as the windings act as a source term in the equations, we do not need to define their conductivity.

Material	Relative permeability	Electrical conductivity (S/m)
Transformer oil	1	1
Aluminium	1	-
Grain-oriented steel	μ_r	σ_{core}

Table 6.1: Material parameters

Since the model is 2D, we need to consider that the core is laminated to prevent eddy current. As mentioned in Section 5.3.2, we can only take into account the laminations in a 2D model by lowering the conductivity of the core. Therefore, it is assumed that $\sigma_{core} = 0.1 \text{ S}/\text{m}$ instead of the approximate value given by JFE Steel of $\sigma = \frac{1}{5e-7} = 2e6 \text{ S}/\text{m}$ [55].

We can model the permeability of the core in different ways, as discussed in Section 5.3.1. To model the losses in the frequency domain, we first consider the effective B-H curve. However, to obtain this curve, we first need a B-H curve. IEO supplied this curve, and by using the B-H curve checker in COMSOL to minimize numerical errors, we obtained the B-H curve in Figure 6.3 [56]. Then with the Effective Nonlinear Magnetic Curves Calculator in COMSOL, we can convert this curve into an effective B-H curve used in frequency domain studies, as shown in Figure 6.4 [51].

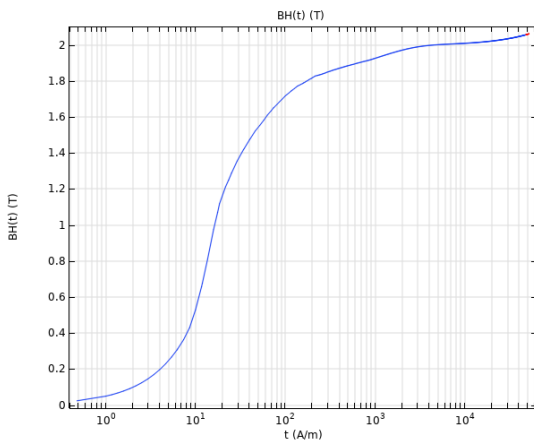


Figure 6.3: B-H curve

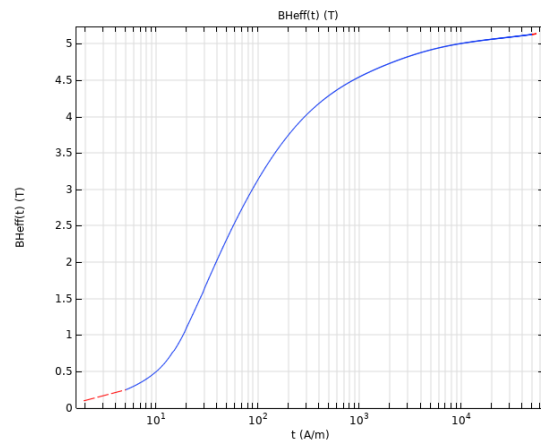


Figure 6.4: Effective B-H curve

The effective B-H curve converges to a value a bit above 5T. At that point, the transformer's core goes into saturation and cannot take in any more magnetic flux.

Lastly, since we are considering a 2D model, we need to imagine the windings going around the core legs. Hence, the current moves in a positive direction on one side of the core leg and in a negative direction on the other side. This direction is given in Figure 6.5, where the yellow coils are going out of the plane, and the black coils are going into the plane.

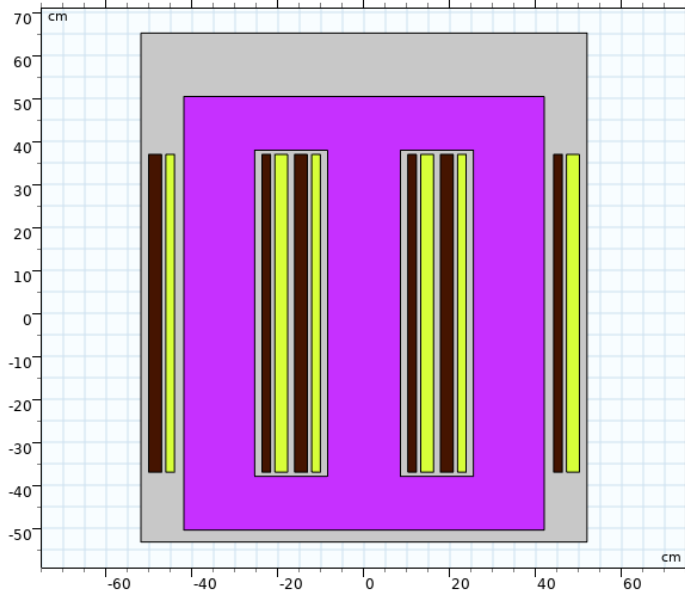


Figure 6.5: Directions of coil excitation. The yellow coils are going out of the plane, and the black coils are going into the plane

With all the parameters at hand, the goal is to approximate the measured values from IEO with the finite element model and expand these losses under different harmonic loads. The measured losses under a non-harmonic load are in Table 6.2. Therefore, we start by modelling the no-load (or core) losses.

	Loss (W)
No-load	358W
Load	2693W

Table 6.2: No-load and load loss determined by IEO, both at $T = 17^\circ\text{C}$

6.4. Core loss

Manufacturers determine the core loss of a transformer by performing an open circuit test. Therefore, they apply a voltage to the secondary, low voltage winding and leave the primary, high voltage side open. By keeping the primary side open, no current will flow through the primary windings as they are not connected. In our model, this means that the following voltages will supply the secondary side, with $V = 342.93V$, as calculated by Equation 6.9:

$$V_{phase,A} = V e^{\frac{2}{3}i\pi}, \quad V_{phase,B} = V, \quad V_{phase,C} = V e^{-\frac{2}{3}i\pi} \quad (6.14)$$

And all windings on the primary side will have $I = 0A$.

Running the model with these parameters gives the real part of the vector potential in Figure 6.6 and the imaginary component of the vector potential in Figure 6.7.

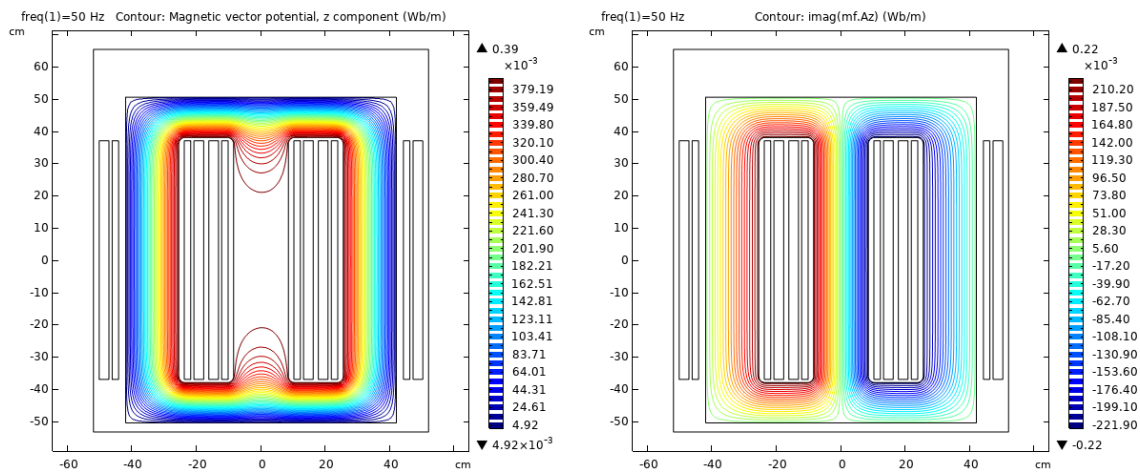


Figure 6.6: The contour of the real part of the vector potential under open-circuit test

Figure 6.7: The contour of the imaginary part of the vector potential under open-circuit test

And with the resulting flux density norm in Figure 6.8.

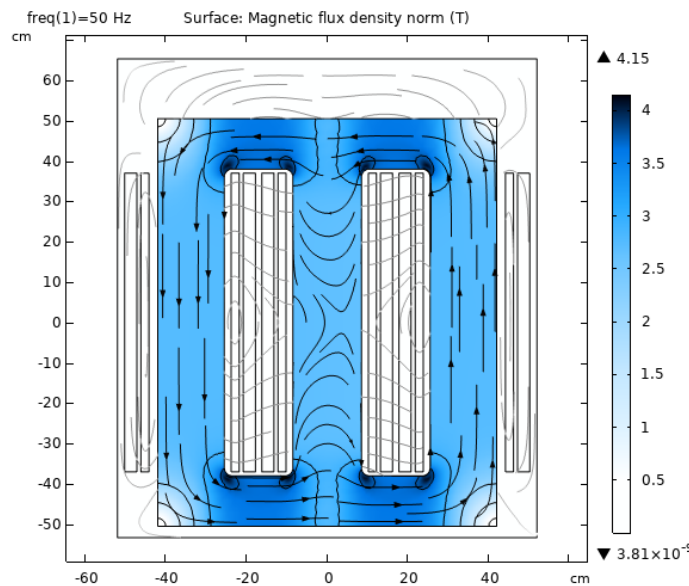


Figure 6.8: Magnetic flux density norm $\|\mathbf{B}\|$ under open-circuit test

As we are not using the complex permeability, we cannot use the COMSOL defined magnetic losses. However, we can use Steinmetz losses. Unfortunately, the documentation of the transformer did not contain the data needed to determine the Steinmetz parameters. So, we have to estimate these. Therefore, let $K_c = 50 \text{ W/m}^3$, $\alpha = 1$ and $\beta = 1.5$. Then a surface integration of Equation 5.49 multiplied with the out of plane thickness L gives $P_{Stmz} = 2855.9 \text{ W}$. This value is still far from the no-load losses given in Table 6.2, so more work needs to be done to estimate these better.

6.5. Winding loss

Manufactures determine the load loss of a transformer using a short circuit test. With such a test, they apply a voltage to one side of the transformer, and connect the wires on the other side to create a short circuit. For the measurements from IEO, they supplied the primary side with a $460.3V$ voltage. This voltage is the line RMS value, so as before:

$$V_{prm,phase,peak} = 460.3 \cdot \sqrt{2} = 650.96V \quad (6.15)$$

So, we will have on the primary side:

$$V_{phase,A} = V e^{\frac{2}{3}i\pi}, \quad V_{phase,B} = V, \quad V_{phase,C} = V e^{-\frac{2}{3}i\pi} \quad (6.16)$$

with $V = 650.96V$.

Now, running this model with the effective B-H curve in Figure 6.4 gives Figure 6.9 and 6.10 for the real and imaginary component of the vector potential \mathbf{A} and Figure 6.11 for the flux density norm $\|\mathbf{B}\|$.

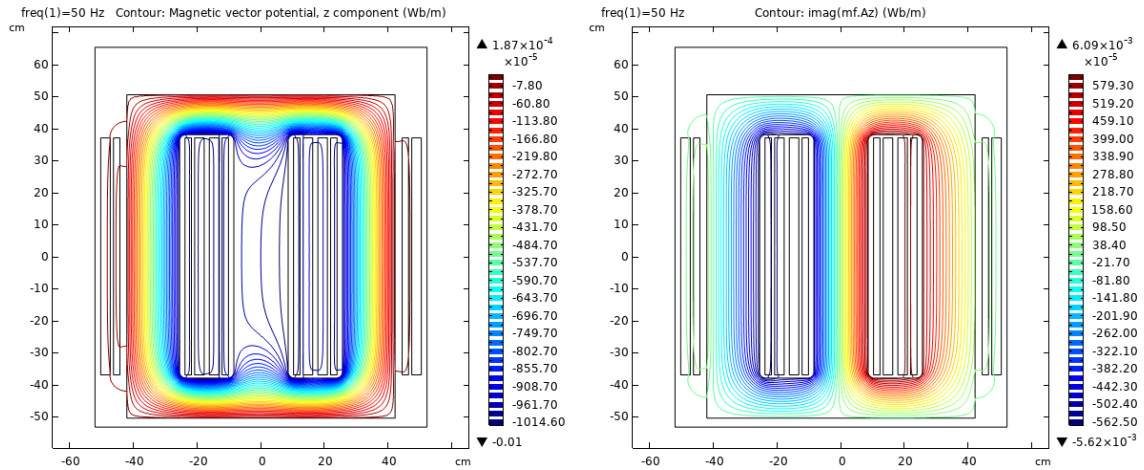


Figure 6.9: The contour of the real part of the vector potential under short circuit test

Figure 6.10: The contour of the imaginary part of the vector potential under short circuit test

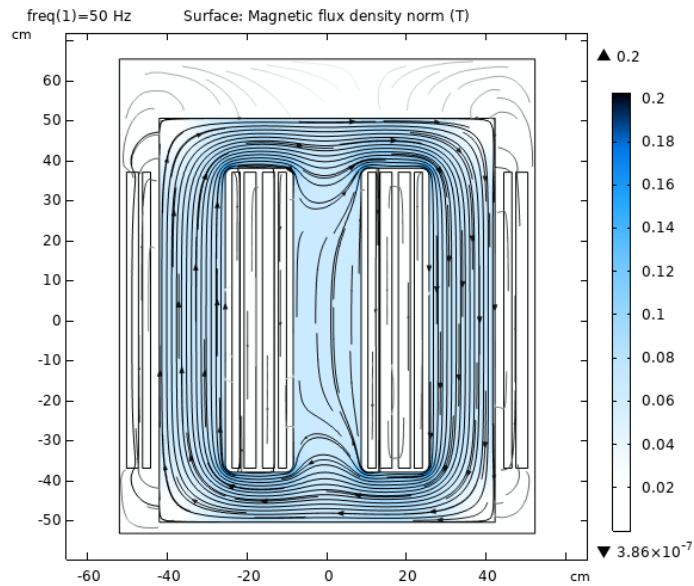


Figure 6.11: Magnetic flux density norm $\|\mathbf{B}\|$ under short circuit test

We can now use Equation 5.57 on the primary coils to compute the winding loss in the primary windings. These are then equal to the load loss given by IEO. So, the losses are $P = 5420.6W$, about twice as much as measured by IEO.

Summarizing both losses gives Table 6.3.

	IEO	Model
No-load	358 W	2855.9 W
Load	2693 W	5420.6 W

Table 6.3: Comparison between the measured losses and theoretically determined losses

6.6. Harmonics

We can repeat both the open and the short circuit test with higher frequencies to calculate the effect of harmonics in the losses. However, we also must consider that the amplitude is lower for higher frequencies. Therefore, we will take the harmonic distribution presented in Figure 2.12 as an example. The core losses resulting from an open circuit test are then equal to:

freq (Hz)	Amplitude	Core loss (W)
50.000	1	2855.9
150.00	0.4	408.77
250.00	0.2	112.08
350.00	0.1	33.510

Table 6.4: Open circuit losses for harmonics

Summing the third column gives the total core losses under the given harmonic distribution: $P = 3410.3 \text{ W}$.

freq (Hz)	Amplitude	I ² R loss (W)
50.000	1	5420.6
150.00	0.4	847.80
250.00	0.2	202.83
350.00	0.1	47.634

Table 6.5: Short circuit losses for harmonics

Summing the second column gives the total winding losses under the given harmonic distribution: $P = 6518.8 \text{ W}$.

So combining the two: the losses have increased from $2855.9 + 5420.6 = 8276.5 \text{ W}$ to 9929.1 W , an increase of almost 20%.

For higher frequencies, we also have to consider the skin effect in the core when meshing the geometry. The skin effect is a physical phenomenon where the distribution of current in a conductive medium changes with higher frequencies. For higher frequencies, the current moves more along the sides of the medium instead of being evenly distributed.

In our model, this effect only occurs in the core, where we have a conductivity of $\sigma = 0.1 \text{ S/m}$. Therefore we need to change the mesh in the core. We, therefore, remove the rounded corners and refine the mesh in the core and windings using the mapped mesh option. With a mapped mesh, the mesh consists of rectangles instead of the triangular shapes in the previous mesh. Additionally, the length and width of the rectangular elements decrease when nearing the core boundary. This is shown in Figure 6.13, where there are two mesh elements between 40 and 41 cm on the y-axis and eight mesh elements between 38 and 39 cm. Figure 6.12 show the complete mesh of the domain.

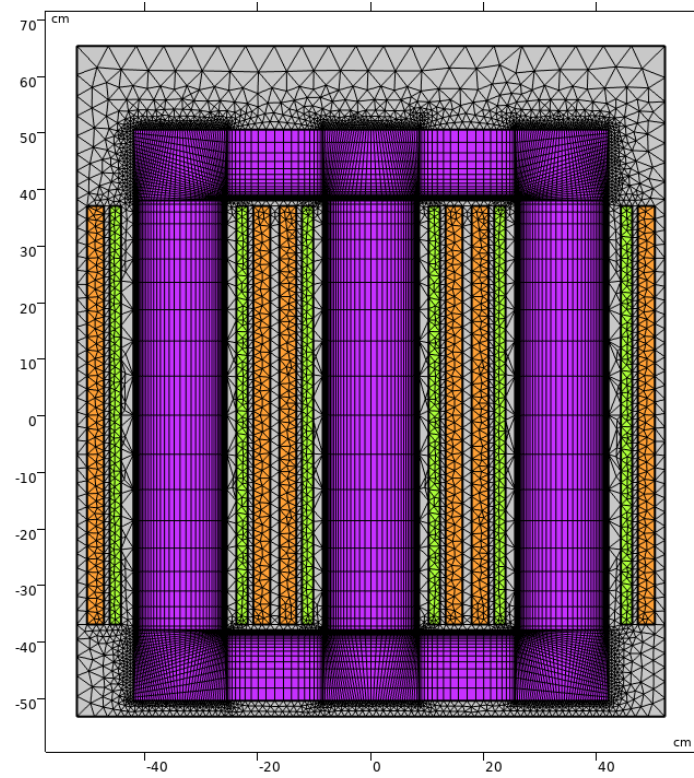


Figure 6.12: Mapped mesh for core legs and windings

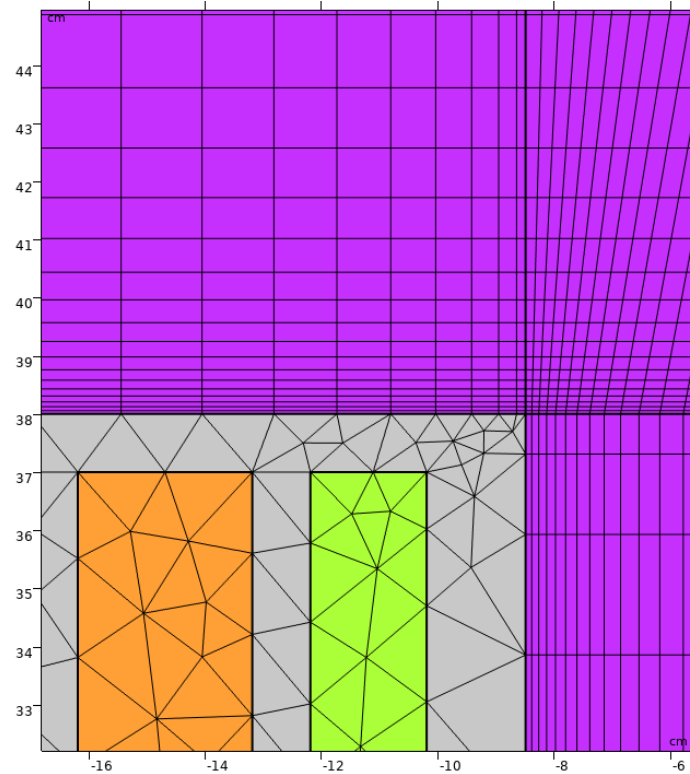


Figure 6.13: Enlarged mesh for the top left of the middle leg of the core

Rerunning the open circuit test with the new mesh gives the losses in the third column of Table 6.6.

freq (Hz)	Amplitude	Old mesh (W)	New mesh (W)
50.000	1	2855.9	2889.1
150.00	0.4	408.77	412.10
250.00	0.2	112.08	112.99
350.00	0.1	33.510	33.783

Table 6.6: Open circuit losses for harmonics

The new model results in a total core loss of $P = 3448.0 \text{ W}$, only slightly higher than the 3410 W with the previous mesh. The losses for the short circuit test give the same results as with the previous mesh.

The losses are the same because the skin effect does not occur with these parameters as the thickness of the current, also called skin depth, is too large. We can calculate this skin depth with the following formula [29]:

$$\delta = \sqrt{\frac{2}{\sigma\omega\mu}} = \frac{1}{\sqrt{\pi f \sigma \mu_r \mu_0}} \quad (6.17)$$

Since we are using an effective B-H curve in our calculations, we can calculate the relative permeability using the following formula:

$$\mu_r = \frac{\mathbf{B}}{\mathbf{H}\mu_0} \quad (6.18)$$

The open-circuit case gives an average relative permeability of $\mu_r = 30000$ for the core. If we have a frequency of $f = 50 \text{ Hz}$, the skin depth is equal to $\delta = 1.30 \text{ m}$ and for $f = 350 \text{ Hz}$ the skin depth is $\delta = 0.49 \text{ m}$. As the width of the core legs is only 0.36 m , there are no skin effects present in the model, and therefore the losses are the same with both meshes.

However, things change if we vary the conductivity of the core, which we previously set at $\sigma_{core} = 0.1 \text{ S/m}$. For example, if we set $\sigma_{core} = 1 \text{ S/m}$ then the skin depth at $f = 350 \text{ Hz}$ is $\delta = 0.15 \text{ m}$, so the effect is visible. The value of the skin depth is also why the mesh elements decrease in size near the boundary; as near the boundary, the skin effect occurs, and we want multiple mesh elements per skin depth. Therefore, if we consider higher frequencies and higher conductivities, we might need to refine the mesh even more, as in that case, the mesh elements might be larger than the skin depth. However, a coarser mesh can still give valid results since we use second-order shape functions in the finite element method.

To visualize the skin effect, we first compute the electromagnetic behaviour at different frequencies with the same amplitude. If we then take a cut line through the middle of the centre core leg, we can plot the conduction current, so the term $J_{cond_z} = \sigma E_z$ in Maxwell's equation, along this cut line at different frequencies and different conductivities in Figure 6.15.

In these figures, a positive current means that the current is coming out of the plane, whereas a negative current is going into the plane. In Figure 6.15a, we see that the lines are almost diagonal for all frequencies, meaning no skin effect occurs. The slight deviation between the lines is due to the asymmetry in the conduction current. We can see this more clearly in Figure 6.14a, where there is more conduction current around the right core window than the left window.

To explain this asymmetry, we need to remember that we excited the coils with balanced voltages, as in Equation 6.14. Here the voltages were all 120° or $\frac{2}{3}\pi$ rad out of phase with one another. However, by multiplying the potential with i in Equation 5.29 and in the frequency domain equation for Equation 5.38, this symmetry is disturbed. This effect is especially visible at the higher core conductivities as there we multiply i with a higher value.

We can see the skin effect most clearly in Figure 6.15d, where we see that the current first rapidly decreases from $7000 A/m^2$ to $-3000 A/m^2$ for higher frequencies, but then increases again to $0 A/m^2$. We can also see this if we compare Figure 6.14a and Figure 6.14b, wherein the left figure shows current in almost the whole core, but in the right figure, the current is only nonzero a small distance away from the core windows.

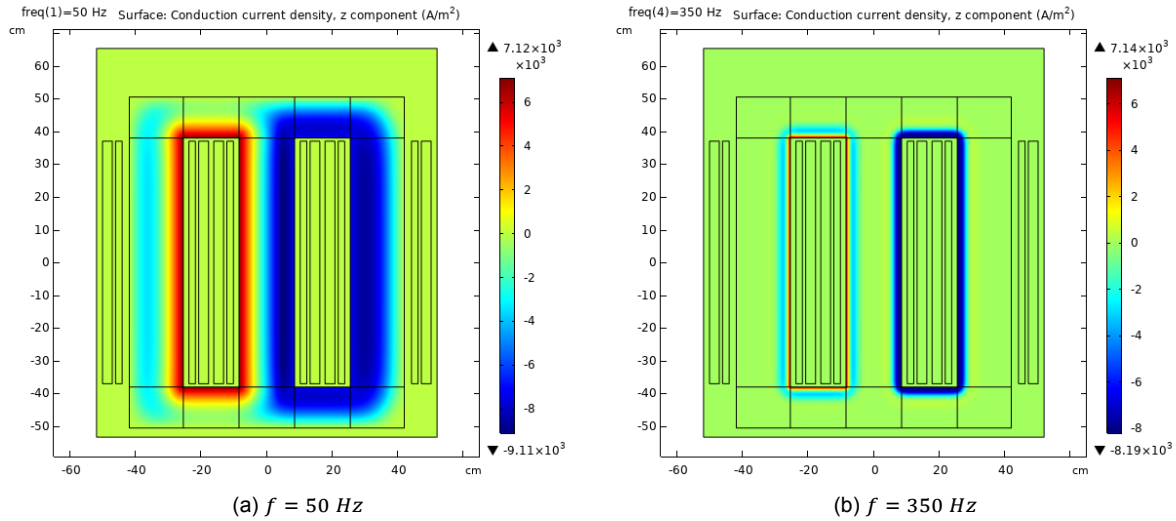


Figure 6.14: The conduction current J_{cond_z} over the whole model for $\sigma_{core} = 100 S/m$

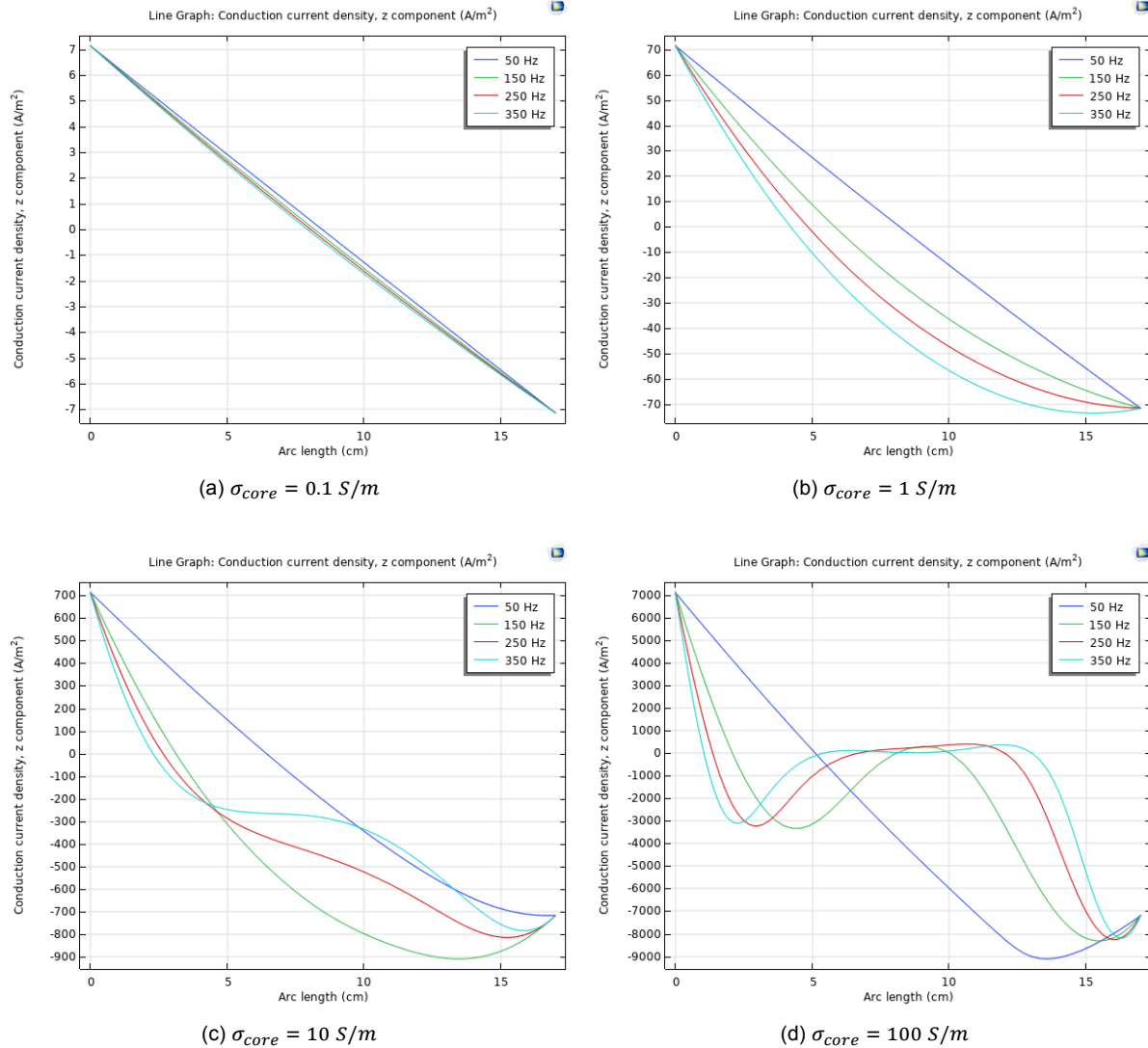


Figure 6.15: The conduction current J_{cond_z} along a cut line through the middle of the centre leg for multiple values of the core conductivity at different frequencies.

7

Discussion & recommendations

7.1. Discussion

In the last chapter, we saw that we could use the finite element method to solve Maxwell's equations and determine both the no-load and load losses of a transformer. This model is a first step towards developing a physics-based digital twin of a distribution transformer with which Stedin can monitor and predict the impact of the energy transition more closely. Section 7.2.2 describes how Stedin could further develop such a digital twin.

However, as Stedin generally does not know the exact internal dimensions and materials in its transformers, particularly for the older transformers, it is not easy to accurately represent the transformer's behaviour. When Stedin knows this, the fundamental approach will give a better overview of what happens inside the transformer than the loading guide, which only estimates the hot spot temperature based on empirical relations.

When considering the impact of harmonics, we calculated the individual losses for every frequency and corresponding amplitude and added them together. However, summing the losses this way is only valid when using a linear permeability in the transformer core. In the current model, we used an effective B-H curve, which is non-linear. As a result, the model could lead to an over-or underestimation of the losses, which in the end affects the loss of life calculations. To fix this problem, one could simulate the real current (the brown/gold curve in Figure 2.12) in the time domain, but this will result in a significantly longer computation time.

7.2. Recommendations

As we did this research in collaboration with Stedin, we will give two types of recommendations: academic recommendations to further improve the model and suggestions for Stedin to use the presented models.

7.2.1. Future research

To further improve the first principles model, we look at a figure presented in Chapter 3 and given again in Figure 7.1. In the model developed in this research, we only covered the top block: the effects of electromagnetic behaviour. However, to precisely determine the condition of transformers, the other blocks also need to be investigated. The most important one of which is heat transfer. The heat transfer can be modelled with the heat equation in Equation 5.59, with the losses as a source term. However, to fully model the heat distribution, we also must consider the transformer's oil flow. By modelling the flow, we can consider the oil's velocity,

density, and viscosity at specific points, all of which affect the final temperature distribution. When considering the temperature distribution inside the transformer, we can determine a hot spot temperature, for example, the maximum over the domain or a fixed point somewhere in the windings. We can then use the same formulas as the loading guide to determine the loss of life with this hot spot temperature.

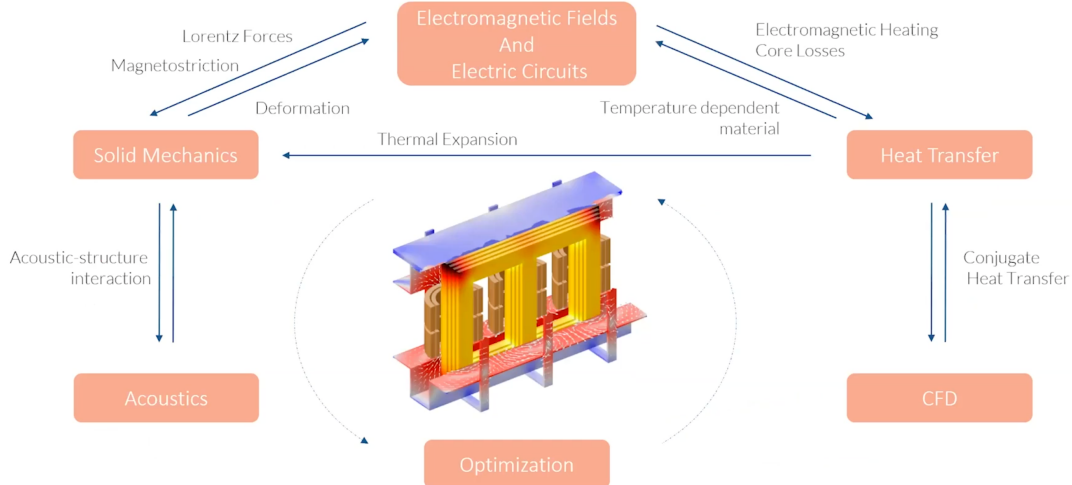


Figure 7.1: Multi-physical behaviour of a transformer [33]

After incorporating the heat into the model, another addition can be the effect of the heat on the materials inside the transformer. For example, the windings have a lower conductivity at higher temperatures, resulting in more losses. Additionally, we can model the paper insulation material. Modelling the paper combined with the oil flow will result in a more accurate estimation of what a particular load will do to the behaviour of a transformer over a more extended time period. One can use homogenization techniques to model the paper insulation without individually modelling the wires, which would be computationally intensive.

We can model the heat transfer and its effect on the materials in 2D. However, a 3D model can be considered a more realistic model as, in that case, we can consider all 3D physical effects, such as 3D electromagnetic behaviour. We have to note here that the computation time in 3D models is often longer than in 2D models. Here we can compare the computation time between our model and the 3D transformer model developed by COMSOL, which only considers the electromagnetic effects [57]. In the open-circuit case (to calculate the no-load losses), their 3D model takes 5 minutes 22 seconds to run on a MacBook Pro (2017), whereas our model only takes 14 seconds.

On the other hand, in the short circuit case, their model takes 1 minute 6 seconds to run, whereas our model only takes 4 seconds. Therefore, to speed up the process in 3D, one needs to look at more refined meshing techniques in, for instance, cfMesh or gmsh. Additionally, one can consider more robust solvers such as Krylov methods.

When considering harmonics, we have to note the influence of super harmonics for this model. Super harmonics have a frequency of at least 40 times the base frequency of 50 Hz. If we want to consider these in our model, we need to refine the mesh, as in that case (with $\sigma_{core} = 1 S/m$ and $\mu_r = 30000$), we will have a skin depth of $6.5 \cdot 10^{-9} m$. Therefore, the mesh needs to be refined such that there are multiple mesh elements within a distance of $6.5 \cdot 10^{-9} m$ from the core boundary.

7.2.2. For Stedin

Suppose we combine the statements made at the end of Chapter 4 and at the beginning of this chapter. In that case, we can conclude that both the loading guide and the finite element model can be valuable additions for Stedin to monitor distribution transformers. For one, the loading guide can give an idea about the temperature with only a few transformer parameters when the load is balanced and sinusoidal. However, a more analytical approach can be helpful for situations when the load is not like this, as the experimentally determined loading guide parameters might no longer be valid under different loading conditions.

After talks with transformer manufacturer IEO and smart monitoring company Withthegrid, we can conclude that the loading guide is practical for transformer monitoring. However, to get the most out of the procedure described in the loading guide, it is vital to measure the top oil temperature of the transformer. With a top oil thermometer, one of the equations in the guide becomes superfluous, which reduces the uncertainty. However, we can also use the data from the top oil thermometer to determine the parameters in this equation. We can then use these determined parameters on similar-looking transformers placed in locations with the same ventilation household, of which we do not measure the temperature. By determining the parameters like this, the loading guide will give a more accurate idea about the hot spot temperature instead of using the standardized parameters. We need similar ventilation households for transformers where we want to measure the top oil temperature on one and use the parameters on the others because the loading guide only considers the ambient temperature as a variable for the environment. In contrast, we can consider the surroundings and ventilation with the finite element method, which will be a future research assignment at Stedin.

Another option to get a more accurate representation of these parameters is to monitor the temperature in the transformer for some time with an infrared camera. An infrared camera gives the temperature distribution over the whole transformer. So, we can set two points for the top oil and hot spot temperature and use these to determine new parameters. We can wrap fibre optic temperature sensors with the windings for newly developed transformers. These fibre optic sensors can measure the temperature at different points in the transformer, giving a completer image of the temperature distribution than the top oil temperature measurement. To account for harmonics in the loading guide, we need to measure the harmonic spectrum with a power quality device and do the calculations presented in Section 4.5.

Stedin can also incorporate the finite element model into their operations. Therefore, to get a complete model, it can follow the same recommendations as given in the previous section by including the heat and other physical behaviour into the model. Additionally, Stedin can consider an extension towards a 3D model to get a complete image of the transformer and consider all the electromagnetic effects. This 3D model can then be validated using the top oil temperature or infrared cameras.

A complete 3D model will be a more realistic asset-based digital twin of a transformer but also more computationally intensive. Therefore, it would not be suitable to serve as part of a grid-based digital twin to calculate the impact of specific changes to the grid. It would also not be a helpful tool to monitor the transformer actively, as the computation time would be too long.

However, when we reduce this 3D model to a much simpler model by removing some parts that appear to be unnecessary for the condition of the transformer, like maybe the carpentry which holds the transformer or the influence of the oil flow, we can reduce the computation time by a lot. We can still validate this simpler model with the data we used to build the complete model and see whether or not it gives satisfactory results. Maybe at this point, we also conclude that a 3D model is too computationally intensive that we go back to a 2D model.

This simpler model can then act as a digital twin of the transformer. By receiving the data from the sensors placed in the transformer room on a small processor, the model can calculate the transformer's temperature and send a message if this temperature has reached a predefined limit. Furthermore, immediately using the data from sensors would save a lot of storage time. Otherwise, the sensors would have to send all the data to a central server where someone would check if the transformer behaves normally. Therefore, this model is an example of using a finite element model in edge computing.

Additionally, this simpler model can be used in a grid-based digital twin to calculate the effect of specific changes to the grid on the transformer. For example, when the government plans to build a data centre or a supermarket, we can use this grid-based twin to calculate beforehand what the expected load pattern would do to the condition of the transformer.

Unfortunately, the program used in this study for finite element simulations, COMSOL, is not suitable for online monitoring as the software is based on licences and can not be easily run on a small processor. Therefore, we must convert the models developed in this study to another program. One option is to use Julia and the Gridap.jl package.

The question remains on which transformers the finite element model is helpful for transformer monitoring or where the loading guide suffices. As the finite element model gives a more accurate representation of the losses under a specific load, Stedin can best use it in areas where the current contains many harmonics. Such as in regions with many renewable energy sources or many electric car chargers since these draw instant power.

8

Conclusion

From the outside, distribution transformers look like a relatively simple asset, and for Stedin, they are. They install them, and the transformer requires minimum inspection and hardly any maintenance during its lifetime in the next 30 to 80 years. However, with the transition to more renewable energy sources, which have a more variable load pattern and the demand for electricity rising, transformers, and especially distribution transformers, become an asset to monitor more closely. In this thesis, we looked at two ways to determine the remaining life of a distribution transformer in the context of digital twins: the more empirical and currently standard approach of the loading guide and a more fundamental approach where we used the finite element method to solve Maxwell's equations to determine the losses in a transformer. With the second approach, the impact of harmonics can be taken into account more accurately than with the loading guide.

For the loading guide, we see that only a few transformer parameters are needed to estimate the hot spot temperature under a specific load. Then, we can use this hot spot temperature to determine the loss of life over the considered period of time. By using the nominal life span of 180.000 hours, we can compare the results to what would normally be the life loss over that period. The problem with this approach is the following: how do you determine all the variables and parameters in the model? The simplest way is to take the parameters written in the loading guide (Table 4.1). However, this does not consider the variety of distribution transformers Stedin currently has. Therefore, the loading guide can result in an over-or underestimation of the remaining lifetime, both cases leading to extra costs. On the other hand, if we measure the top oil temperature, we can determine the parameters by curve fitting Equation 4.6. We can then use these new parameters to monitor similar distribution transformers of which the top oil temperature is unavailable.

Another problem with figuring out which parameters to use in the loading guide is the sensitivity of the exponents x and y . Since these are exponents, a slight change in value will result in a significant difference in the final result, as was observed in Figure 4.5. This difference makes it even harder to get accurate results with this basic set of functions. Furthermore, the exponents have a crucial effect when considering higher loads on a transformer. For those higher loads, a slight change in exponent can lead to a big change in temperature, resulting in a significant difference in the loss of life since an exponential function also gives the ageing acceleration factor.

According to the new standard to include harmonics in the loading guide, including harmonics only changes the variables of temperature rise, whereas observing the physical behaviour of transformers paints a different picture: the effects of harmonics are mainly present in the extra losses. Furthermore, with the method in the standard, we saw in Figure 4.6 that with the given harmonic distribution, the transformer's lifespan decreases drastically, further indicating that harmonics have a significant impact on the loss of life.

Considering all statements mentioned above, we can conclude that the loading guide is a viable option to determine the loss of life for transformers that meet the following requirements: the top oil temperature is available, and the harmonic load on the transformer is only small.

We can use the more analytical approach for transformers that do not meet these requirements. By modelling the transformer in this way, we saw that with a limited amount of data on the geometry of the transformer and some transformer parameters, we made a model that gives an estimate of both the no-load and the load losses, as given in Table 8.1. In this table, we see that we are still quite far from the measured losses, but this model can serve as the first step towards a physics-driven digital twin of a transformer as described in Section 7.2.2. Furthermore, we extended these losses to include the theoretical impact of harmonics instead of the more empirically derived effects as calculated with the loading guide.

	IEO	Model
No-load	358 W	2855.9 W
Load	2693 W	5420.6 W

Table 8.1: Comparison between the measured losses and theoretically determined losses

To answer the starting question, is it possible to model analogue assets in a digital twin? The answer is yes. For most transformers, we can model their loss of life with the loading guide, which only requires the load on the transformer to be measured and the top oil temperature on some transformers. However, the loading guide is insufficient for transformers dealing with harmonic loading patterns and unbalanced loads. In those instances, we can use a more analytical approach based on Maxwell's equations to accurately determine the losses. Then with future development of the model, the heat distribution and, therefore, the loss of life can be analytically determined.

Bibliography

- [1] M. Sugiyama, "Climate change mitigation and electrification", en, *Energy Policy*, vol. 44, pp. 464–468, May 2012, ISSN: 0301-4215. DOI: 10.1016/j.enpol.2012.01.028. [Online]. Available: <https://www.sciencedirect.com/science/article/pii/S030142151200033X> (visited on 25/10/2021).
- [2] PricewaterhouseCoopers Advisory N.V., "De energietransitie en de financiële impact voor netbeheerders", Tech. Rep., Jul. 2021. [Online]. Available: <https://www.netbeheernederland.nl/nieuws/pwc-rapport-tijdige-ombouw-energiesysteem-in-gevaar-door-onvoldoende-financieringsmogelijkheden-1448> (visited on 30/11/2021).
- [3] M. Muratori, M. Alexander, D. Arent, M. Bazilian, P. Cazzola, E. M. Dede, J. Farrell, C. Gearhart, D. Greene, A. Jenn, M. Keyser, T. Lipman, S. Narumanchi, A. Pesaran, R. Sioshansi, E. Suomalainen, G. Tal, K. Walkowicz and J. Ward, "The rise of electric vehicles—2020 status and future expectations", en, vol. 3, no. 2, p. 022002, Mar. 2021, Publisher: IOP Publishing, ISSN: 2516-1083. DOI: 10.1088/2516-1083/abe0ad. [Online]. Available: <https://doi.org/10.1088/2516-1083/abe0ad> (visited on 14/11/2021).
- [4] K. Muthanna, A. Sarkar, K. Das and K. Waldner, "Transformer insulation life assessment", *IEEE Transactions on Power Delivery*, vol. 21, no. 1, pp. 150–156, Jan. 2006, Conference Name: IEEE Transactions on Power Delivery, ISSN: 1937-4208. DOI: 10.1109/TPWRD.2005.855474.
- [5] P. Palensky, M. Cvetkovic, D. Gusain and A. Joseph, "Digital twins and their use in future power systems", en, *Digital Twin*, vol. 1, p. 4, Sep. 2021, ISSN: 2752-5783. DOI: 10.12688/digitaltwin.17435.1. [Online]. Available: <https://digitaltwin1.org/articles/1-4/v1> (visited on 15/11/2021).
- [6] M. M. Armstrong, *Cheat sheet: What is Digital Twin? Internet of Things blog*, en-US, Dec. 2020. [Online]. Available: <https://www.ibm.com/blogs/internet-of-things/iot-cheat-sheet-digital-twin/> (visited on 24/09/2021).
- [7] M. Van Nuland, *Bouwen aan een digitale tweeling van het elektriciteitsnet*, nl-NL. [Online]. Available: <https://www.tudelft.nl/ewi/actueel/nodes/bouwen-aan-een-digitale-tweeling-van-het-elektriciteitsnet> (visited on 24/09/2021).
- [8] H. Silva and A. L. Soares, "Digital Platforms as Enablers of Smart Product-Service Systems", en, Nov. 2021, 8p. [Online]. Available: <https://hal-emse.ccsd.cnrs.fr/emse-03346190> (visited on 13/10/2021).
- [9] Mathworks, *Digital Twins for Predictive Maintenance*. [Online]. Available: <https://explore.mathworks.com/digital-twins-for-predictive-maintenance/chapter-04-36US-761YW.html> (visited on 13/10/2021).
- [10] L. Wright and S. Davidson, "How to tell the difference between a model and a digital twin", *Advanced Modeling and Simulation in Engineering Sciences*, vol. 7, no. 1, p. 13, Mar. 2020, ISSN: 2213-7467. DOI: 10.1186/s40323-020-00147-4. [Online]. Available: <https://doi.org/10.1186/s40323-020-00147-4> (visited on 13/10/2021).

- [11] P. G. Madhavan, "Stochastic Formulation of Causal Digital Twin: Kalman Filter Algorithm", *arXiv:2105.05236 [cs, eess]*, May 2021, arXiv: 2105.05236. [Online]. Available: <http://arxiv.org/abs/2105.05236> (visited on 13/10/2021).
- [12] D. J. Griffiths, *Introduction to Electrodynamics*, en, ISBN: 9781108333511 Publisher: Cambridge University Press, Jun. 2017. DOI: 10.1017/9781108333511. [Online]. Available: <https://www.cambridge.org/highereducation/books/introduction-to-electrodynamics/3AB220820DBB628E5A43D52C4B011ED4> (visited on 07/10/2021).
- [13] P. v. Oirsouw, *Netten voor distributie van elektriciteit*, Dutch. 2012, OCLC: 848914616, ISBN: 978-90-817983-1-0.
- [14] MBizon, *Electricity Grid Schematic English*, Mar. 2010. [Online]. Available: https://commons.wikimedia.org/wiki/File:Electricity_Grid_Schematic_English.svg (visited on 31/10/2021).
- [15] ABB, *Transformer Handbook*. Feb. 2004. (visited on 20/10/2021).
- [16] *Different Types of Transformers*, en-US, Jul. 2019. [Online]. Available: <https://www.electpower.com/types-of-transformers/> (visited on 14/09/2021).
- [17] D. Gebouwd, *Vegeta: Distributietransformator op plantaardige olie*, nl, Dec. 2008. [Online]. Available: <https://www.duurzaamgebouwd.nl/artikel/20081218-vegeta-distributietransformator-op-plantaardige-olie> (visited on 25/10/2021).
- [18] HyperPhysics, *Magnetic Field of a Current Loop*, 2017. [Online]. Available: <http://hyperphysics.phy-astr.gsu.edu/hbase/magnetic/curloo.html#c3> (visited on 22/10/2021).
- [19] Sumiran Satsangi, "Transformer Core Market by Transformer Type (Power Transformer, Distribution Transformer, and Others) - Global Opportunity Analysis and Industry Forecast, 2014-2022", en, Tech. Rep., Sep. 2016. [Online]. Available: <https://www.alliedmarketresearch.com/transformer-core-market> (visited on 21/10/2021).
- [20] James H. Harlow, *Electric Power Transformer Engineering*. Jun. 2012, vol. Third Edition, ISBN: 978-1-4398-5629-1. (visited on 01/11/2021).
- [21] SpinningSpark, *English: Transformer core, (transferred from WP:en)*, Mar. 2012. [Online]. Available: https://commons.wikimedia.org/wiki/File:Transformer_winding_formats.jpg (visited on 17/08/2021).
- [22] J. C. Olivares-Galván, F. d. León, P. S. Georgilakis and R. Escarela-Pérez, "Selection of copper against aluminium windings for distribution transformers", en, *IET Electric Power Applications*, vol. 4, no. 6, pp. 474–485, Jul. 2010, Publisher: IET Digital Library, ISSN: 1751-8679. DOI: 10.1049/iet-epa.2009.0297. [Online]. Available: <https://digital-library.theiet.org/content/journals/10.1049/iet-epa.2009.0297> (visited on 11/11/2021).
- [23] H. De Gersem and K. Hameyer, "A finite element model for foil winding simulation", *IEEE Transactions on Magnetics*, vol. 37, no. 5, pp. 3427–3432, Sep. 2001, Conference Name: IEEE Transactions on Magnetics, ISSN: 1941-0069. DOI: 10.1109/20.952629.
- [24] K. Daware, *Three Phase Transformer Connections*, May 2014. [Online]. Available: <https://www.electricleeasy.com/2014/05/three-phase-transformer-connections.html> (visited on 22/10/2021).
- [25] "Transformer Insulation Materials and Ageing", en, in *Transformer Ageing*, Tapan Kumar Saha and Prithviraj Purkait, Eds., John Wiley & Sons, Ltd, 2017, pp. 1–33, ISBN: 978-1-119-23997-0. DOI: 10.1002/9781119239970.ch1. [Online]. Available: <http://>

- / / onlinelibrary.wiley.com / doi / abs / 10 . 1002 / 9781119239970 . ch1 (visited on 21/10/2021).
- [26] *35KV Dry Type Dry Cast Resin Transformers SCB10 Dry Type Power Transformer*. [Online]. Available: <http://www.electrical-power-transformer.com/sale-12826147-35kv-dry-type-dry-cast-resin-transformers-scb10-dry-type-power-transformer.html> (visited on 02/11/2021).
- [27] J.C. Das, *Power System Analysis: Short-Circuit Load Flow and Harmonics, Second Edition*, en. Apr. 2017, ISBN: 978-1-138-07504-7. [Online]. Available: <https://www.routledge.com/Power-System-Analysis-Short-Circuit-Load-Flow-and-Harmonics-Second-Edition/Das/p/book/9781138075047> (visited on 21/10/2021).
- [28] J. J. Grainger and W. D. Stevenson, *Power system analysis*, eng, ser. McGraw-Hill series in electrical and computer engineering Power and energy. New York: McGraw-Hill, 1994, OCLC: 29224990, ISBN: 978-0-07-113338-8.
- [29] M. H. Rashid, Ed., *Power Electronics Handbook*, English, 4th edition. Oxford: Butterworth-Heinemann, Oct. 2017, ISBN: 978-0-12-811407-0.
- [30] Chetvorno, *Laminated core eddy currents 2.svg - Wikipedia*, nl, Mar. 2016. [Online]. Available: https://commons.wikimedia.org/wiki/File:Laminated_core_eddy_currents_2.svg (visited on 06/10/2021).
- [31] M. Getzlaff, "Magnetization Dynamics", en, in *Fundamentals of Magnetism*, M. Getzlaff, Ed., Berlin, Heidelberg: Springer, 2008, pp. 133–149, ISBN: 978-3-540-31152-2. DOI: 10.1007/978-3-540-31152-2_9. [Online]. Available: https://doi.org/10.1007/978-3-540-31152-2_9 (visited on 14/12/2021).
- [32] D. S. Takach and R. L. Boggavarapu, "Distribution Transformer No-Load Losses", *IEEE Transactions on Power Apparatus and Systems*, vol. PAS-104, no. 1, pp. 181–193, Jan. 1985, Conference Name: IEEE Transactions on Power Apparatus and Systems, ISSN: 0018-9510. DOI: 10.1109/TPAS.1985.318892.
- [33] Roman Obrist, *Analyzing Transformer Designs Using COMSOL Multiphysics®*. [Online]. Available: <https://www.comsol.com/video/analyzing-transformer-designs-using-comsol-multiphysics>.
- [34] IEC, *IEC 60076-7:2018 Power transformers - Part 7: Loading guide for mineral-oil-immersed power transformers*, Jan. 2018. [Online]. Available: <https://webstore.iec.ch/publication/34351>.
- [35] R. Khalili Senobari, J. Sadeh and H. Borsi, "Frequency response analysis (FRA) of transformers as a tool for fault detection and location: A review", en, *Electric Power Systems Research*, vol. 155, pp. 172–183, Feb. 2018, ISSN: 0378-7796. DOI: 10.1016/j.epsr.2017.10.014. [Online]. Available: <https://www.sciencedirect.com/science/article/pii/S0378779617304200> (visited on 30/11/2021).
- [36] IEEE Power & Energy Society, "IEEE Guide for Loading Mineral-Oil-Immersed Overhead and Pad-Mounted Distribution Transformers Rated 500kVA and Less with 65 C or 55 C Average Winding Rise", in *ANSI/IEEE Std C57.91-1981*, Jul. 1981, pp. 1–26. DOI: 10.1109/IEEESTD.1981.81014.
- [37] J. Ramadan, A. Alkeesh and K. Kosha, "Thermal Model for Calculating Transformer Hot-Spot Temperature Using IEC Loading Guide", 2018.
- [38] L. Wang, X. Zhang, R. Villarroel, Q. Liu, Z. Wang and L. Zhou, "Top-oil temperature modelling by calibrating oil time constant for an oil natural air natural distribution transformer", English, *IET Generation, Transmission & Distribution*, vol. 14, no. 20, pp. 4452–4458, Oct. 2020, Publisher: Institution of Engineering and Technology, ISSN: 1751-8687. DOI: 10.1049/iet-gtd.2020.0155. [Online]. Available: <https://www.researchgate.net/publication/34351>.

- manchester.ac.uk / portal / en / publications / topoil - temperature - modelling - by - calibrating - oil - time - constant - for - an - oil - natural - air - natural - distribution - transformer (58a2ae9b - fd1a - 4ec3 - a638 - b8671d3ba95c) .html (visited on 17/01/2022).
- [39] B. Kuspan, M. Bagheri, O. Abedinia, M. S. Naderi and E. Jamshidpour, "The Influence of Electric Vehicle Penetration on Distribution Transformer Ageing Rate and Performance", in *2018 7th International Conference on Renewable Energy Research and Applications (ICRERA)*, ISSN: 2572-6013, Oct. 2018, pp. 313–318. DOI: 10.1109/ICRERA.2018.8566966.
- [40] Working Group A2.24, "Thermal Performance of Transformers", EN, *CIGRE Tech. Brochure No. 393*, 2009. [Online]. Available: https://e-cigre.org/publication/ELT_246_4-thermal-performance-of-transformers (visited on 12/01/2022).
- [41] IEEE Power & Energy Society, "IEEE Guide for Loading Mineral-Oil-Immersed Transformers and Step-Voltage Regulators", in *IEEE Std C57.91-2011 (Revision of IEEE Std C57.91-1995)*, Jul. 2012, pp. 1–123. DOI: 10.1109/IEEESTD.2012.6166928.
- [42] D. Susa, *Dynamic thermal modelling of power transformers*, en. Helsinki University of Technology, Aug. 2005, Accepted: 2012-02-17T07:04:44Z ISSN: 1795-4584, ISBN: 978-951-22-7742-1. [Online]. Available: <https://aalto.doc.aalto.fi:443/handle/123456789/2584> (visited on 06/12/2021).
- [43] T. Prevost, "Thermally upgraded insulation in transformers", in *Proceedings Electrical Insulation Conference and Electrical Manufacturing Expo, 2005.*, ISSN: 2334-0975, Oct. 2005, pp. 120–125. DOI: 10.1109/EEIC.2005.1566272.
- [44] IEEE Power & Energy Society, "IEEE Standard for General Requirements for Liquid-Immersed Distribution, Power, and Regulating Transformers", in *IEEE Std C57.12.00-2015 (Revision of IEEE Std C57.12.00-2010)*, Conference Name: IEEE Std C57.12.00-2015 (Revision of IEEE Std C57.12.00-2010), May 2016, pp. 1–74. DOI: 10.1109/IEEESTD.2016.7469278.
- [45] S. Najar, J.-F. Tissier, S. Cauet and E. Etien, "Improving thermal model for oil temperature estimation in power distribution transformers", en, *Applied Thermal Engineering*, vol. 119, pp. 73–78, Jun. 2017, ISSN: 1359-4311. DOI: 10.1016/j.applthermaleng.2017.03.061. [Online]. Available: <https://www.sciencedirect.com/science/article/pii/S1359431117317015> (visited on 10/12/2021).
- [46] IEEE Power & Energy Society, "IEEE Recommended Practice for Establishing Liquid-Immersed and Dry-Type Power and Distribution Transformer Capability When Supplying Nonsinusoidal Load Currents", in *IEEE Std C57.110™-2018 (Revision of IEEE Std C57.110-2008)*, Oct. 2018, pp. 1–68. DOI: 10.1109/IEEESTD.2018.8511103.
- [47] S. W. Ellingson, *Electromagnetics, Volume 1*, en. VT Publishing, Aug. 2018, Accepted: 2018-08-16T16:36:21Z, ISBN: 978-0-9979201-9-2. DOI: 10.21061/electromagnetics-vol-1. [Online]. Available: <https://vttechworks.lib.vt.edu/handle/10919/84164> (visited on 15/12/2021).
- [48] J. P. A. Bastos and N. Sadowski, *Electromagnetic Modeling by Finite Element Methods*, English, 1st edition. New York: CRC Press, Apr. 2003, ISBN: 978-0-8247-4269-0.
- [49] O. Ozgun and M. Kuzuoglu, *MATLAB-based finite element programming in electromagnetic modeling*, English. 2019, OCLC: 1050437377, ISBN: 978-0-429-45739-5. [Online]. Available: <http://search.ebscohost.com/login.aspx?direct=true&scope=site&db=nlebk&db=nlabk&AN=1878839> (visited on 07/09/2021).
- [50] *Magnetic Hysteresis Loop including the B-H Curve*, en, Aug. 2013. [Online]. Available: <https://www.electronics-tutorials.ws/electromagnetism/magnetic-hysteresis.html> (visited on 14/12/2021).

- [51] COMSOL, *Effective Nonlinear Magnetic Curves Calculator*, en. [Online]. Available: <https://www.comsol.com/model/effective-nonlinear-magnetic-curves-calculator-30941> (visited on 02/12/2021).
- [52] C. Steinmetz, "On the law of hysteresis", *Proceedings of the IEEE*, vol. 72, no. 2, pp. 197–221, Feb. 1984, Conference Name: Proceedings of the IEEE, ISSN: 1558-2256. DOI: 10.1109/PROC.1984.12842.
- [53] COMSOL, *AC/DC Module - User's Guide*, 2020. [Online]. Available: <https://doc.comsol.com/5.6/doc/com.comsol.help.acdc/ACDCModuleUsersGuide.pdf>.
- [54] *Three Phase Transformer Connections and Basics*, en, Sep. 2013. [Online]. Available: <https://www.electronics-tutorials.ws/transformer/three-phase-transformer.html> (visited on 22/12/2021).
- [55] JFE Steel Corporation, *Electrical Steel Sheets, JFE G-CORE, JFE N-CORE*. [Online]. Available: <https://www.jfe-steel.co.jp/en/products/electrical/catalog/f1e-001>. (visited on 22/11/2021).
- [56] COMSOL, *B-H Curve Checker*, en. [Online]. Available: <https://www.comsol.com/model/b-h-curve-checker-71651> (visited on 02/12/2021).
- [57] Neena Picardo, *Computing Losses in a Three-Phase Power Transformer*, en, Feb. 2021. [Online]. Available: <https://www.comsol.com/blogs/computing-losses-in-a-three-phase-power-transformer/> (visited on 02/08/2021).

A

Dataset example Loading Guide

T (min)	Power (VA)	K	T (min)	Power (VA)	K	T (min)	Power (VA)	K
0	90632	0.2266	480	84496	0.2112	960	145885	0.3647
5	87384	0.2185	485	90890	0.2272	965	141841	0.3546
10	84981	0.2125	490	93163	0.2329	970	139837	0.3496
15	83146	0.2079	495	98108	0.2453	975	133386	0.3335
20	84907	0.2123	500	99597	0.2490	980	136887	0.3422
25	87725	0.2193	505	98362	0.2459	985	136639	0.3416
30	79928	0.1998	510	91869	0.2297	990	154286	0.3857
35	76180	0.1904	515	93731	0.2343	995	151985	0.3800
40	77039	0.1926	520	94716	0.2368	1000	155044	0.3876
45	76792	0.1920	525	97118	0.2428	1005	159394	0.3985
50	74368	0.1859	530	105147	0.2629	1010	158899	0.3972
55	74622	0.1866	535	104003	0.2600	1015	157197	0.3930
60	71622	0.1791	540	107183	0.2680	1020	164701	0.4118
65	70942	0.1774	545	113028	0.2826	1025	172480	0.4312
70	70002	0.1750	550	110422	0.2761	1030	168362	0.4209
75	72007	0.1800	555	111861	0.2797	1035	174832	0.4371
80	72160	0.1804	560	112962	0.2824	1040	189962	0.4749
85	73781	0.1845	565	119073	0.2977	1045	186822	0.4671
90	73299	0.1832	570	119010	0.2975	1050	191992	0.4800
95	70458	0.1761	575	122689	0.3067	1055	191082	0.4777
100	69528	0.1738	580	124603	0.3115	1060	187498	0.4687
105	67436	0.1686	585	132496	0.3312	1065	185998	0.4650
110	65099	0.1627	590	132009	0.3300	1070	192771	0.4819
115	68469	0.1712	595	128700	0.3218	1075	199496	0.4987
120	67036	0.1676	600	129576	0.3239	1080	206517	0.5163
125	68210	0.1705	605	127413	0.3185	1085	204387	0.5110
130	63990	0.1600	610	127804	0.3195	1090	210256	0.5256
135	64769	0.1619	615	127175	0.3179	1095	211271	0.5282
140	65689	0.1642	620	128202	0.3205	1100	206229	0.5156
145	64307	0.1608	625	128392	0.3210	1105	204244	0.5106
150	66597	0.1665	630	124125	0.3103	1110	208867	0.5222
155	63096	0.1577	635	123259	0.3081	1115	202881	0.5072
160	59182	0.1480	640	125620	0.3141	1120	196694	0.4917
165	58900	0.1472	645	125307	0.3133	1125	192270	0.4807
170	60564	0.1514	650	120001	0.3000	1130	196534	0.4913
175	62440	0.1561	655	120804	0.3020	1135	196641	0.4916
180	58725	0.1468	660	129948	0.3249	1140	189261	0.4732
185	59660	0.1491	665	141164	0.3529	1145	189679	0.4742
190	61890	0.1547	670	139799	0.3495	1150	184082	0.4602
195	59996	0.1500	675	138177	0.3454	1155	181740	0.4544
200	64307	0.1608	680	140124	0.3503	1160	187187	0.4680
205	66058	0.1651	685	141334	0.3533	1165	184782	0.4620
210	63745	0.1594	690	149980	0.3750	1170	175533	0.4388
215	62121	0.1553	695	148521	0.3713	1175	175258	0.4381
220	60181	0.1505	700	144376	0.3609	1180	173667	0.4342
225	60308	0.1508	705	141417	0.3535	1185	173318	0.4333
230	60196	0.1505	710	147581	0.3690	1190	169773	0.4244
235	61040	0.1526	715	146777	0.3669	1195	164371	0.4109
240	59301	0.1483	720	149909	0.3748	1200	168221	0.4206
245	58038	0.1451	725	148055	0.3701	1205	172753	0.4319
250	58805	0.1470	730	144272	0.3607	1210	178325	0.4458
255	59824	0.1496	735	144121	0.3603	1215	182975	0.4574
260	63883	0.1597	740	149576	0.3739	1220	173717	0.4343
265	63937	0.1598	745	145084	0.3627	1225	167163	0.4179
270	62170	0.1554	750	142663	0.3567	1230	166068	0.4152
275	62263	0.1557	755	137850	0.3446	1235	163899	0.4097
280	60921	0.1523	760	138402	0.3460	1240	165171	0.4129
285	62470	0.1562	765	133722	0.3343	1245	161625	0.4041
290	60876	0.1522	770	139069	0.3477	1250	154074	0.3852
295	60829	0.1521	775	137292	0.3432	1255	150885	0.3772
300	56347	0.1409	780	143127	0.3578	1260	147604	0.3690
305	56444	0.1411	785	137475	0.3437	1265	145720	0.3643
310	60787	0.1520	790	140858	0.3521	1270	151881	0.3797
315	60513	0.1513	795	136541	0.3414	1275	154515	0.3863
320	62441	0.1561	800	141014	0.3525	1280	149288	0.3732
325	63779	0.1594	805	145866	0.3647	1285	145118	0.3628
330	62694	0.1567	810	145047	0.3626	1290	141291	0.3532
335	61864	0.1547	815	142160	0.3554	1295	138023	0.3451
340	61118	0.1528	820	138318	0.3458	1300	137351	0.3434
345	58742	0.1469	825	139422	0.3486	1305	138649	0.3466
350	61753	0.1544	830	147283	0.3682	1310	134897	0.3372
355	60028	0.1501	835	148331	0.3708	1315	135034	0.3376
360	60001	0.1500	840	146226	0.3656	1320	133546	0.3339
365	59832	0.1496	845	135171	0.3379	1325	129685	0.3242
370	60720	0.1518	850	131572	0.3289	1330	128611	0.3215
375	62742	0.1569	855	135912	0.3398	1335	127927	0.3198
380	64365	0.1609	860	133564	0.3339	1340	126386	0.3160
385	64251	0.1606	865	132518	0.3313	1345	123860	0.3096
390	64092	0.1602	870	132838	0.3321	1350	123352	0.3084
395	63768	0.1594	875	132573	0.3314	1355	121414	0.3035
400	62834	0.1571	880	135798	0.3395	1360	118307	0.2958
405	63927	0.1598	885	139291	0.3482	1365	113386	0.2835
410	66008	0.1650	890	137862	0.3447	1370	107898	0.2697
415	67496	0.1687	895	135939	0.3398	1375	108025	0.2701
420	69995	0.1750	900	137367	0.3434	1380	104757	0.2619
425	71633	0.1791	905	137791	0.3445	1385	102287	0.2557
430	70026	0.1751	910	135398	0.3385	1390	99321	0.2483
435	73333	0.1833	915	136744	0.3419	1395	95813	0.2395
440	77614	0.1940	920	138080	0.3452	1400	91969	0.2299
445	76481	0.1912	925	136249	0.3406	1405	90982	0.2275
450	76353	0.1909	930	137401	0.3435	1410	91450	0.2286
455	78662	0.1967	935	128948	0.3224	1415	89325	0.2233
460	78769	0.1969	940	127316	0.3183	1420	87064	0.2177
465	81500	0.2037	945	129416	0.3235	1425	85848	0.2146
470	85532	0.2138	950	132984	0.3325	1430	79196	0.1980
475	82698	0.2067	955	137682	0.3442	1435	81028	0.2026

B

Complex losses

Why is there a factor $\frac{1}{2}$ in front of Equation 5.56, but not in front of Equation 5.55?

Let \mathbf{Y} and \mathbf{Z} two harmonic fields in the time domain with a different phase angle ϕ , so:

$$\mathbf{Y} = \begin{bmatrix} y \cdot \sin(2\pi \cdot 50 \cdot t) \\ y \cdot \sin(2\pi \cdot 50 \cdot t + \frac{2}{3}\pi) \\ y \cdot \sin(2\pi \cdot 50 \cdot t - \frac{2}{3}\pi) \end{bmatrix} \quad \mathbf{Z} = \begin{bmatrix} z \cdot \sin(2\pi \cdot 50 \cdot t + \phi) \\ z \cdot \sin(2\pi \cdot 50 \cdot t + \frac{2}{3}\pi + \phi) \\ z \cdot \sin(2\pi \cdot 50 \cdot t - \frac{2}{3}\pi + \phi) \end{bmatrix} \quad (\text{B.1})$$

With ϕ in radians. Then:

$$\mathbf{Y} \cdot \mathbf{Z} = y \sin(2\pi \cdot 50 \cdot t) \cdot z \sin(2\pi \cdot 50 \cdot t + \phi) \quad (\text{B.2})$$

$$+ y \sin(2\pi \cdot 50 \cdot t + \frac{2}{3}\pi) \cdot z \sin(2\pi \cdot 50 \cdot t + \frac{2}{3}\pi + \phi) \quad (\text{B.3})$$

$$+ y \sin(2\pi \cdot 50 \cdot t - \frac{2}{3}\pi) \cdot z \sin(2\pi \cdot 50 \cdot t - \frac{2}{3}\pi + \phi) \quad (\text{B.4})$$

$$= \frac{3}{2}yz \cos(\phi) \quad (\text{B.5})$$

However, if we do the same in the frequency domain, so:

$$\mathbf{Y} = \begin{bmatrix} y \cdot \exp(2\pi i \cdot 50 \cdot t) \\ y \cdot \exp(2\pi i \cdot 50 \cdot t + \frac{2}{3}\pi i) \\ y \cdot \exp(2\pi i \cdot 50 \cdot t - \frac{2}{3}\pi i) \end{bmatrix} \quad \mathbf{Z} = \begin{bmatrix} z \cdot \exp(2\pi i \cdot 50 \cdot t + i\phi) \\ z \cdot \exp(2\pi i \cdot 50 \cdot t + \frac{2}{3}\pi i + i\phi) \\ z \cdot \exp(2\pi i \cdot 50 \cdot t - \frac{2}{3}\pi i + i\phi) \end{bmatrix} \quad (\text{B.6})$$

Then:

$$\operatorname{Re}(\mathbf{Y} \cdot \bar{\mathbf{Z}}) = \operatorname{Re}(y \exp(2\pi i \cdot 50 \cdot t) \cdot z \exp(-2\pi i \cdot 50 \cdot t - i\phi)) \quad (\text{B.7})$$

$$+ y \exp(2\pi i \cdot 50 \cdot t + \frac{2}{3}\pi i) \cdot z \exp(-2\pi i \cdot 50 \cdot t - \frac{2}{3}\pi i - i\phi) \quad (\text{B.8})$$

$$+ y \exp(2\pi i \cdot 50 \cdot t - \frac{2}{3}\pi i) \cdot z \exp(-2\pi i \cdot 50 \cdot t + \frac{2}{3}\pi i - i\phi) \quad (\text{B.9})$$

$$= 3yz \cos(\phi) \quad (\text{B.10})$$

So this only results in the same answer if we multiply the harmonic case with $\frac{1}{2}$.

C

Abstract presented at SCEE conference

Remaining Life Assessment of Distribution Transformers via Digital Twins

M. van Dijk¹, J.D. Schuddebeurs², and D.J.P. Lahaye¹

¹ TU Delft, The Netherlands m.vandijk-5@student.tudelft.nl, D.J.P.Lahaye@tudelft.nl

² Stedin, The Netherlands Jeroen.Schuddebeurs2@stedin.net

Summary. In this research, we investigated two models to determine the condition of distribution transformers in the context of digital twins: the loading guide and a finite element model based on quasi-stationary Maxwell equations. The loading guide only takes balanced harmonic excitations into account. The finite element method extends modelling capabilities to non-balanced non-harmonic loads. Such loads are expected to occur more frequently in distribution grids.

1 Introduction

The shift towards more renewable energy sources and the increase of large loads, such as electric vehicles, has a significant impact on the assets currently in the grid. These ageing assets will be prone to more and often more variable loads. These changes in load can cause the loss of life (LoL) of assets to increase faster than anticipated. One category of assets that has to deal with these issues is distribution transformers. As distribution transformers are installed in every neighbourhood, they have to deal with the different electromagnetic behaviour coming from power converters between photovoltaic panels and electrical vehicles (harmonics) and the more load they cause [3]. More load and more harmonics mean more losses, which results in higher transformer temperatures and greater LoL. Therefore, there is a need for monitoring the distribution transformers more closely. To fully monitor these transformers and make predictions about their LoL and hence remaining life (RL), the idea of a digital twin for distribution transformers is investigated here.

2 Loss of Life in a Digital Twin

The loading guide has been devised to determine the condition of transformers without on-site visits [1]. It uses the normalized load, ambient temperature, and some transformer parameters to estimate the hot-spot temperature. Then, the LoL can be calculated with the hot spot temperature over a period.

However, the loading guide only considers the hot spot temperature in a transformer when the load is balanced, and the voltages and currents are sinusoidal.

Because of harmonics, this is often not the case, and these harmonics cause extra heat. Therefore, a 2D finite element model of a transformer was developed to more accurately monitor these aspects [2]. With this model, the individual losses under a certain load and harmonic spectrum can be calculated, which can later be used in a multi-physics coupling to determine the heat distribution. With the multi-physics coupling, a physics-based digital twin can be made to more accurately determine the heat distribution inside the transformer. Furthermore, as the model is 2D, it can easily be solved on a small processor (edge computing) in the transformer room, enabling the RL assessment of a transformer in the context of digital twins. Then, when the losses increase rapidly or the temperature reaches a limit, a signal can be sent to the asset manager to check what is happening.

3 Conclusions

As the load on distribution transformers is increasing and phenomena such as harmonics have a significant impact on the temperature in the transformer, more monitoring needs to be done. Placing sensors requires substantial investments, so models have to be made to estimate the temperature with which the LoL of transformers can be determined. These models can be validated with measurements on one transformer, and since distribution transformers are relatively similar, these models can be extended to a whole collection of transformers.

References

1. IEC. IEC 60076-7:2018, January 2018.
2. M. van Dijk. A theoretical approach towards digital twins. Master's thesis, TU Delft, Delft, 2022.
3. John Wamburu et al. Analyzing distribution transformers at city scale and the impact of evs and storage. In *Proceedings of the Ninth International Conference on Future Energy Systems*, e-Energy '18, page 157–167, New York, NY, USA, 2018. Association for Computing Machinery.